Peatland warming influences the abundance and distribution of branched tetraether lipids: Implications for temperature reconstruction

Nicholas O E Ofiti, Arnaud Huguet, Paul J Hanson, Guido L B Wiesenberg

Science of the Total Environment 924 (2024) 171666

Contents lists available at ScienceDirect

Science of the Total Environment

journal homepage: www.elsevier.com/locate/scitotenv

Peatland warming influences the abundance and distribution of branched tetraether lipids: Implications for temperature reconstruction

Nicholas O.E. Ofiti [a,b,*], Arnaud Huguet [c], Paul J. Hanson [d], Guido L.B. Wiesenberg [a]

[a] Department of Geography, University of Zurich, Zurich, Switzerland
[b] CEREEP-Ecotron Ile De France, ENS, CNRS, PSL Research University, Saint-Pierre-lès-Nemours, France
[c] Sorbonne Université, CNRS, EPHE, PSL, UMR METIS, Paris, France
[d] Environmental Sciences Division and Climate Change Science Institute, Oak Ridge National Laboratory, Oak Ridge, TN, USA

HIGHLIGHTS

- BrGDGTs were measured under varying degrees of in-situ warming in a boreal peatland.
- Depth-specific response of brGDGT lipids to warming
- The methylation of brGDGTs is affected strongly by rising soil temperatures.
- Changes in brGDGT signal reflect predominance of physiological adaptation of brGDGT- producing bacteria.

GRAPHICAL ABSTRACT

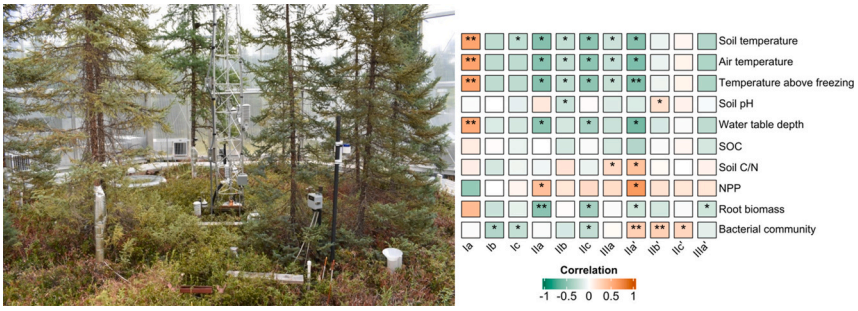

ARTICLE INFO

Editor: Jose Julio Ortega-Calvo

Keywords:
Peatland
Warming
Branched GDGTs
Lipid biomarkers
Bacterial community
Paleoclimate proxies

ABSTRACT

Branched glycerol dialkyl glycerol tetraethers (brGDGTs) are bacterial membrane lipids whose distribution in peatland soils serves as an important proxy for past climate changes due to strong linear correlations with temperature in modern environments. However, commonly used brGDGT-based temperature models are characterized by high uncertainty (ca. 4 °C) and these calibrations can show implausible correlations when applied at an ecosystem level. This lack of accuracy is often attributed to our limited understanding of the exact mechanisms behind the relationship between brGDGTs and temperature and the potential effect of temperature-independent factors on brGDGT distribution. Here, we examine the abundance and distribution of brGDGTs in a boreal peatland after four years of in-situ warming (+0, +2.25, +4.5, +6.75 and +9 °C). We observed that with warming, concentrations of total brGDGTs increased. Furthermore, we determined a shift in brGDGT distribution in the surface aerobic layers of the acrotelm (0–30 cm depth), whereas no detectable change was observed at deeper anaerobic depths (>40 cm), possibly due to limited microbial activity. The response of brGDGTs to warming was also reflected by a strong increase in the methylation index of 5-methyl brGDGTs (MBT'_{5Me}), classically used as a temperature proxy. Further, the relationship between the MBT'_{5Me} index and soil temperature differed between 0–10, 10–20 and 20–30 cm depth, highlighting depth-specific response of brGDGTs to warming, which should be considered in paleoenvironmental and paleoecological studies. As the bacterial community composition was generally unaltered, the rapid changes in brGDGT distribution argue for a physiological adaptation of the microorganisms producing these lipids. Finally, soil temperature and water table depth

* Corresponding author at: Department of Geography, University of Zurich, Zurich, Switzerland.
E-mail address: nicholas.ofiti@geo.uzh.ch (N.O.E. Ofiti).

https://doi.org/10.1016/j.scitotenv.2024.171666
Received 25 October 2023; Received in revised form 16 February 2024; Accepted 10 March 2024
Available online 13 March 2024

were better predictors of brGDGT concentration and distribution, highlighting the potential for these drivers to impact brGDGT-based proxies. To summarize, our results provide insights on the response of brGDGT source microorganisms to soil warming and underscore brGDGTs as viable temperature proxies for better understanding of climatic perturbation in peatlands.

1. Introduction

Northern peatlands store a significant fraction of terrestrial soil carbon, estimated at one-third of the global soil carbon pool (Gorham, 1991; Bridgham et al., 2006; Yu, 2012). This results from the slow process of organic matter accumulation that has been taking place over millennia under predominantly waterlogged conditions and minimal bioturbation (Moore and Basiliko, 2006; Yu et al., 2010). However, there is considerable concern that climate-driven changes are likely to modify carbon storage (Bradford et al., 2016; Gallego-Sala et al., 2018), but the underlying mechanisms and their interactions, particularly those resulting in increased organic matter decomposition, are still unknown (Gauthier et al., 2015; Chaudhary et al., 2020). An improved understanding of peatland response to environmental perturbations and future dynamics of these ecosystems is possible from studying their Holocene history. In particular, peat archives have been used to reconstruct climatic changes throughout the Holocene using a wide array of proxies including plant macrofossils, pollen, and organic biomarkers (e.g., Pancost et al., 2002; Charman et al., 2013; Nichols et al., 2014; Zheng et al., 2015; Coffinet et al., 2018; Rao et al., 2021), providing key information on past and ongoing global changes. Of these biomarkers, branched glycerol dialkyl glycerol tetraethers (brGDGTs) have emerged as increasingly popular proxies for understanding past climatic changes, partly because they are globally ubiquitous in terrestrial and aquatic ecosystems (Sinninghe Damste et al., 2000; Weijers et al., 2006; Peterse et al., 2009; Huguet et al., 2013).

BrGDGTs are a suite of membrane-spanning lipids whose structures consists of two alkyl chains, each containing a variable number (and position) of methyl groups (2–4) and cyclopentane moieties (0–2), the latter formed through internal cyclisation (Sinninghe Damste et al., 2000; Weijers et al., 2006; De Jonge et al., 2013, 2014a; Hopmans et al., 2016). Studies have shown that the number of alkyl-chain methylations correlates strongly with temperature on both global and spatial scale (Weijers et al., 2007; De Jonge et al., 2014a; Naafs et al., 2017; Raberg et al., 2022). Similarly, a correlation has been observed between pH and brGDGT cyclopentane ring number (De Jonge et al., 2014a; Naafs et al., 2017). This has led to the development of empirical indices such as the methylation index of 5-methyl branched tetraethers (MBT'_{5Me}) and cyclisation ratio of branched tetraethers (CBT) as paleo-environmental indicators due to strong linear correlations between MBT'_{5Me} and mean annual air temperature and between CBT and soil pH (De Jonge et al., 2014a; Naafs et al., 2017; Dearing Crampton-Flood et al., 2020). Subsequent studies have generally upheld these simple (linear) relationships but have also found important differences in the proxies across ecosystems and regions (Raberg et al., 2022). These discrepancies have led to the use of Bayesian statistics and machine learning algorithms to investigate the relationship between brGDGTs and temperature instead of the classically applied linear regressions (Dearing Crampton-Flood et al., 2020; Véquaud et al., 2022; Häggi et al., 2023). Nevertheless, despite refinements in the brGDGT-based temperature calibrations, the residual scatter in commonly used brGDGT models developed for terrestrial settings remains high (>4 °C).

This uncertainty can be attributed partly to our limited understanding of the exact mechanism behind the relationship between brGDGTs and environmental parameters (Sinninghe Damsté et al., 2018; De Jonge et al., 2019; Raberg et al., 2022; Halamka et al., 2023). While early studies proposed that the empirical relationships between brGDGTs and temperature were physiological adjustments of the membrane lipid composition of source organisms to a changing environment (Weijers et al., 2007; Véquaud et al., 2021), subsequent work challenged this view by demonstrating that this relationship could also reflect restructuring of brGDGT-producer microbial community to a changing environment (Weber et al., 2018; De Jonge et al., 2019; Wu et al., 2021; Raberg et al., 2022). Numerous studies have used incubation and field experiments to test this hypothesis, with varying and often inconclusive results (Huguet et al., 2013; De Jonge et al., 2019; Liang et al., 2019; Halffman et al., 2022; Halamka et al., 2023). Some studies have found that the relative abundance of brGDGTs reflect indirect responses of microorganisms to changes in resource composition and supply, whose effects manifest through restructuring of the bacterial community structure, the so-called “community effect” (Weber et al., 2018; De Jonge et al., 2019; Wu et al., 2021). Other studies have supported physiological adaptation of brGDGT source organisms to temperature via change in methylation of 5-methylated brGDGTs but leaving open the possibility of microbial community-driven pH response (Naafs et al., 2021; Chen et al., 2022; Halamka et al., 2023). Nevertheless, the hypotheses (physiological adjustment vs. community effect) remain impossible to ascertain as the brGDGT source organisms remain incompletely identified and cultured. Based on environmental samples and cultures it has been suggested that brGDGTs are synthesized by bacteria, with at least part of them belonging to the phylum Acidobacteria (Sinninghe Damsté et al., 2011; Chen et al., 2022; Halamka et al., 2023). Furthermore, all of the commonly measured 5-methyl brGDGTs have been detected in two strains of Acidobacteria (Chen et al., 2022; Halamka et al., 2023), which goes one step further than before in the identification of the brGDGT source organisms. Nevertheless, it is unlikely that the same species synthesize all the individual brGDGTs in the different types of terrestrial settings, as the genetic potential to form membrane-spanning lipids is widespread in bacteria (Zeng et al., 2022).

While temperature exerts a strong influence on brGDGT production due to a direct influence on the growth environment of the brGDGT source organisms (De Jonge et al., 2019; Guo et al., 2022), studies have shown that other environmental factors beyond soil temperature and pH have potentially important effects on brGDGT distributions (Huguet et al., 2013; Dang et al., 2016; Liang et al., 2019; Halamka et al., 2021; Halffman et al., 2022). Confounding factors such as thermal regime (seasonality), varying pH conditions, water content, vegetation type, and nutrient status may additionally affect brGDGT distribution, in turn masking relationships with temperature (Huguet et al., 2013; Dang et al., 2016; Liang et al., 2019; Halamka et al., 2021; Guo et al., 2022; Halffman et al., 2022; Rao et al., 2022; De Jonge et al., 2024). Despite efforts to disentangle the potential impacts of these factors in regulating brGDGT production and composition (e.g., Huguet et al., 2013; Liang et al., 2019; Halamka et al., 2021; Halffman et al., 2022; Rao et al., 2022; De Jonge et al., 2024), to date, only a few field warming studies have assessed the reliability of brGDGT-based proxies and confounding factors that, next to temperature, exert an influence on brGDGT distributions (i.e., Huguet et al., 2013; De Jonge et al., 2019, 2021). These in situ warming studies report offsets between MBT'_{5Me} and temperature when vegetation, nutrient status, soil moisture, or seasonality change in peatland (Huguet et al., 2013) and grassland ecosystems (De Jonge et al., 2019, 2021). Importantly, when applied to peatland ecosystems, brGDGT-based temperature proxies show very large errors (which can exceed 10 °C) compared to those of corresponding pollen- and ice core-based temperature records (Dang et al., 2016), suggesting additional influences other than temperature (Rao et al., 2022; Liang et al., 2023). Since key biotic and abiotic factors such as hydrology (water saturation),

plant and microbial community composition and functioning react quickly to alterations in peatland temperature (Wilson et al., 2021; Bucher et al., 2023; Ofiti et al., 2023), it is likely that these confounding factor(s) have an important influence on brGDGT-based climate proxies. Consequently, the mechanistic link between these environmental variables and brGDGTs in peatlands has to be further assessed given the established significance of peatlands as climate archives (Pancost et al., 2002; Nichols et al., 2014; Zheng et al., 2015; Rao et al., 2021).

Here, we investigate the dependency of brGDGTs on peat soil temperature and clarify the potential effect of temperature-independent factors on brGDGTs in a boreal peatland characterized by waterlogged conditions, low temperatures, and acidic pH. Specifically, we assessed the abundance and distribution of brGDGTs following four years of warming at one of the first multi-year, in-situ peatland manipulation experiment (SPRUCE: Spruce and Peatland Responses Under Changing Environments). The experiment is unique in that it provides a powerful climate change gradient that incorporates above- and belowground warming (whole-ecosystem warming; +0, +2.25, +4.5, +6.75, +9 °C above ambient) (Hanson et al., 2017). Given that experiments directly manipulating above- and belowground temperatures are rare, and most studies only allow 1–2 °C warming (Gill et al., 2017), this unique setup of increasing temperatures allows for the evaluation of both direct and indirect effects of temperature on brGDGTs across mild to extreme scenarios for warming. To date, findings at the SPRUCE experiment suggest that warming has resulted in lower water levels during summer dry periods (Hanson et al., 2020) and increased fine-root growth (Malhotra et al., 2020). However, the bacterial community composition has been generally unaltered (Kolton et al., 2019; Wilson et al., 2021). In this study, we utilized datasets from the SPRUCE experiment on vegetation, soil moisture, and bacterial community composition coupled with brGDGT lipid analyses to fully assess the basis for the brGDGT responses to changes in temperature and the applicability of the brGDGT-based temperature proxy in peatlands.

2. Materials and methods

2.1. Study site and experimental setup

The Spruce and Peatland Response Under Changing Environments (SPRUCE) is a multifactorial peatland experiment located on the Marcell Experimental Forest in northern Minnesota, at the southern boundary of the boreal region (47°30′20.5"N, 93°27′12.6"W; http://mnspruce.ornl.gov/). The site has a mean annual air temperature and precipitation of 3.4 °C and 780 mm, respectively (1961–2010) (Sebestyen et al., 2011). This ombrotrophic peatland has accumulated over the last 11,000 years to peat depths of 2–3 m, with a pH ranging from 4.1 to 5.1 (in water solution) (Parsekian et al., 2012; McFarlane et al., 2018). The bog has a typical microtopography (hummock and hollow) and a perched water table. The nominal boundary between the acrotelm (surface aerobic layer) and catotelm (anoxic layer below the water table) fluctuates about 10–20 cm above the hollows after snowmelt, receding deeper later in the growing season (Tfaily et al., 2014; Hobbie et al., 2016; Iversen et al., 2018). The experiment consists of ten octagonal open-top enclosures, 12 m in diameter and 7 m in height installed around existing vegetation dominated by overstory trees, *Picea mariana* and *Larix laricina*, and ericaceous shrubs, *Rhododendron groenlandicum* and *Chamaedaphne calyculata*, above a bryophyte layer, primarily *Sphagnum* mosses. The enclosures are maintained at a series of increasing temperatures to five warming levels (+0, +2.25, +4.5, +6.75 and +9 °C) down to a depth of ~3 m using concentric arrays of electrical resistance heaters installed into peat and forced air warming (Hanson et al., 2017). Peat warming was initiated in 2014, while air warming was established in August 2015, thereby achieving whole ecosystem warming.

2.2. Peat sampling and characterization

In August 2018, two peat cores were taken at random locations within each of the plots in hollow microtopography where the surface of the hollow was defined as 0 cm. Surface samples (0–30 cm) were cut using a stainless-steel knife and extracted by hand, while a Russian peat corer (7.5 cm diameter) was used to sample deeper peat (30–200 cm). Once collected, duplicate cores from the same plot were sectioned by depth (into 10 cm increments over 0 to 50 cm depth and 25 cm intervals from 50 to 200 cm), homogenized and combined to form a mixed sample. The samples were placed into plastic bags and stored frozen at −20 °C immediately after sampling. Peat samples were then freeze-dried, passed through a 5 mm sieve to remove larger litter fragments and ground to a homogenous powder using a ball mill (MM400, Retsch, Haan, Germany). Overall, organic carbon concentration increased with increasing depth from 44.0 % at the surface to 52.5 % at 2 m depth, but there was no effect of temperature on the carbon concentration at any soil depth (Ofiti et al., 2022). The pH of the peat samples was measured in duplicates (at Oak Ridge National Laboratory) on 1 g of milled peat in both 0.01 M calcium chloride solution (Table 1) and water solution (1:2.5 weight ratio) (mean measurement error was 0.01 pH units) (Hanson et al., 2016).

2.3. Branched GDGT extraction and analysis

Solvent extractable compounds (total lipids) were first extracted from ~2 g of milled peat material using standard Soxhlet extraction with dichloromethane (DCM):methanol (MeOH) (93:7; v/v) (Wiesenberg and Gocke, 2017). An aliquot of the total lipid extract was kept for GDGT analyses. Branched GDGTs were separated from total lipids as described by Coffinet et al. (2014). Briefly, total lipid extracts were sequentially separated using column chromatography into apolar and polar fractions using an activated aluminium oxide (Al_2O_3) column, by eluting consecutively with hexane:DCM (9:1; v/v), and DCM:MeOH (1:1; v/v), respectively. The polar fraction, containing the brGDGTs, was re-dissolved in hexane:isopropanol (99:1; v/v) and centrifuged. Prior to analysis, C_{46} GDGT standard was added to the supernatant as an injection standard (Huguet et al., 2013). The GDGTs were analysed using high performance liquid chromatography (HPLC) coupled to mass spectrometry (HPLC-MS) equipped with an atmospheric pressure chemical ionization source (HPLC-APCI-MS, Shimadzu LCMS 2020, Shimadzu Corp.) as described by Huguet et al. (2019). Individual GDGT compounds were identified, integrated and semi-quantified as previously described (Huguet et al., 2013; Coffinet et al., 2014). Overall, analytical errors of the whole process (extraction, separation, and analysis) were typically <10 % based on replicate analysis. The concentrations of the 15 brGDGT lipids are represented as fractional abundances in Fig. S1.

The brGDGT distribution patterns were further summarized using brGDGT-based proxies (De Jonge et al., 2014a; Naafs et al., 2017). The degree of methylation of 5-methyl brGDGTs (MBT'_{5Me}) and 6-methyl brGDGTs (MBT'_{6Me}) were calculated following De Jonge et al. (2014a) (Eqs. (1) and (2)).

$$MBT_{5\acute{M}e} = \frac{[Ia] + [Ib] + [Ic]}{[Ia] + [Ib] + [Ic] + [IIa] + [IIb] + [IIc] + [IIIa]} \quad (1)$$

$$\mathrm{MBT}_{6\acute{M}e} = \frac{[\mathrm{Ia}] + [\mathrm{Ib}] + [\mathrm{Ic}]}{[\mathrm{Ia}] + [\mathrm{Ib}] + [\mathrm{Ic}] + [\mathrm{IIa}] + [\mathrm{IIb}] + [\mathrm{IIc}] + [\mathrm{IIIa}]} \quad (2)$$

The mean annual air temperature was reconstructed using the global soil calibration by De Jonge et al. (2014a) (Eq. (3)). The air temperature was further reconstructed using the only currently available peat-specific calibration (Naafs et al., 2017) (Eq. (4)).

$$\mathrm{MAT} = -8.57 + 31.45 \times \mathrm{MBT}_{5\acute{M}e} \quad (3)$$

Table 1
Environmental conditions in the experimental enclosures. Fractional abundance (%) of brGDGTs present across all samples, and summed concentration of all brGDGTs (μg g^{-1} soil). BrGDGT-based climate ratios 5-methyl (MBT'_{5Me}), the relative abundance of 6-methyl versus 5-methyl brGDGTs (IR_{6Me}) and the cyclization of branched tetraethers index (CBT′).

Plot#	Nominal warming	Depth (cm)	Soil pH	BrGDGT fractional abundance (%)														BrGDGT (μg·g^{-1} soil)	MBT'_{5me}	CBT′	IR'_{6me}
	(°C)		(–)	Ia	Ib	Ic	IIa	IIb	IIc	IIIa	IIIb	IIIc	IIa′	IIb′	IIc′	IIIa′	IIIb′	IIIc′				
6	+0	0–10	3.55	60.41	2.18	1.83	30.77	0.95	0.72	1.81	b.d.l	b.d.l	0.90	0.00	0.00	0.44	b.d.l	b.d.l	0.62	0.65	−1.47	0.04
6	+0	10–20	3.31	58.60	0.96	0.72	33.31	0.63	0.36	3.82	0.01	b.d.l	1.41	0.03	0.01	0.10	b.d.l	0.03	39.06	0.61	−1.62	0.04
6	+0	20–30	3.08	57.89	1.07	0.68	32.56	0.60	0.49	4.37	b.d.l	0.01	2.09	0.02	0.04	0.12	0.01	0.04	80.66	0.61	−1.5	0.06
6	+0	30–40	3.05	58.48	1.20	0.54	35.85	0.12	0.09	2.39	b.d.l	b.d.l	1.22	0.00	0.00	0.11	b.d.l	b.d.l	265.06	0.61	−1.71	0.03
6	+0	40–50	3.04	58.79	2.39	1.68	31.26	0.42	0.42	1.99	0.01	0.01	2.76	0.05	0.05	0.14	0.01	b.d.l	467.79	0.65	−1.29	0.08
6	+0	50–75	3.03	60.18	2.59	1.49	30.71	0.58	0.39	2.02	0.01	0.01	1.77	0.03	0.01	0.18	0.02	0.01	447.13	0.66	−1.42	0.06
20	+2.25	0–10	3.49	65.68	1.35	0.82	27.71	0.45	0.35	1.61	0.34	b.d.l	1.28	0.13	0.14	0.14	b.d.l	b.d.l	3.17	0.69	−1.58	0.05
20	+2.25	10–20	3.38	60.73	0.82	0.57	32.25	0.46	0.27	3.15	0.03	b.d.l	1.51	0.02	0.01	0.14	0.01	0.03	40.75	0.63	−1.62	0.05
20	+2.25	20–30	3.11	60.02	0.79	0.67	32.10	0.60	0.39	3.78	0.02	b.d.l	1.42	0.02	0.01	0.16	b.d.l	0.01	96.22	0.63	−1.62	0.04
20	+2.25	30–40	3.04	60.11	1.29	0.84	32.32	0.53	0.41	2.76	0.01	0.01	1.36	0.10	0.06	0.18	0.01	0.03	292.25	0.63	−1.57	0.05
20	+2.25	40–50	3.03	62.97	1.88	1.74	30.19	0.44	0.40	1.60	0.01	0.01	0.59	0.02	0.01	0.14	b.d.l	b.d.l	560.53	0.67	−1.58	0.02
20	+2.25	50–75	3.05	58.36	2.30	1.37	32.35	0.73	0.42	2.67	0.01	0.01	1.53	0.06	0.01	0.15	0.01	0.01	539.57	0.63	−1.47	0.05
13	+4.5	0–10	3.60	68.73	0.66	0.40	28.04	0.22	0.17	0.79	0.17	b.d.l	0.63	0.06	0.07	0.07	b.d.l	b.d.l	6.48	0.7	−1.9	0.03
13	+4.5	10–20	3.37	62.60	1.24	0.57	32.42	0.39	0.20	1.91	0.04	b.d.l	0.49	0.03	0.00	0.11	b.d.l	b.d.l	41.94	0.65	−1.9	0.02
13	+4.5	20–30	3.38	61.77	1.29	0.82	31.42	0.58	0.55	2.81	0.02	b.d.l	0.59	0.00	0.02	0.13	b.d.l	b.d.l	93.49	0.64	−1.79	0.02
13	+4.5	30–40	3.28	60.56	0.95	0.95	32.02	0.57	0.53	3.41	0.02	b.d.l	0.89	0.01	0.01	0.08	b.d.l	b.d.l	288.71	0.63	−1.69	0.03
13	+4.5	40–50	3.23	62.74	1.42	1.49	27.09	0.43	0.36	2.17	0.02	0.01	4.06	0.07	0.05	0.07	0.01	0.02	465.67	0.69	−1.2	0.12
13	+4.5	50–75	3.27	60.93	2.56	1.49	30.51	0.54	0.41	2.00	0.01	0.01	1.34	0.03	0.01	0.15	0.01	0.01	481.34	0.66	−1.49	0.04
8	+6.75	0–10	3.36	68.68	0.94	0.74	25.89	0.46	0.24	1.79	b.d.l	b.d.l	1.14	0.03	0.03	0.06	b.d.l	b.d.l	18.25	0.71	−1.68	0.04
8	+6.75	10–20	3.23	62.17	0.97	0.65	30.85	0.64	0.29	2.99	b.d.l	b.d.l	1.24	0.03	0.02	0.11	b.d.l	0.05	71.68	0.65	−1.66	0.04
8	+6.75	20–30	3.14	61.58	1.02	0.81	30.28	0.69	0.41	3.65	b.d.l	b.d.l	1.26	0.03	0.12	0.13	b.d.l	0.03	104.41	0.64	−1.6	0.04
8	+6.75	30–40	3.17	60.19	1.51	1.01	32.76	0.54	0.41	2.80	0.01	b.d.l	0.65	0.02	0.01	0.10	b.d.l	b.d.l	342.23	0.63	−1.73	0.02
8	+6.75	40–50	3.15	62.72	1.21	1.10	29.74	0.52	0.49	2.68	0.01	0.01	1.35	0.05	0.00	0.10	0.02	0.00	551.04	0.66	−1.56	0.04
8	+6.75	50–75	3.12	64.60	2.76	1.75	25.98	0.72	0.45	1.71	0.02	b.d.l	1.75	0.03	0.00	0.22	b.d.l	b.d.l	577.83	0.71	−1.39	0.06
17	+9	0–10	3.38	70.31	1.40	0.96	23.99	0.54	0.33	1.65	b.d.l	b.d.l	0.72	0.03	0.02	0.05	b.d.l	b.d.l	17.18	0.73	−1.73	0.03
17	+9	10–20	3.25	63.64	1.02	0.68	29.48	0.58	0.31	3.18	b.d.l	b.d.l	1.01	0.02	0.01	0.06	b.d.l	b.d.l	74.93	0.66	−1.73	0.03
17	+9	20–30	3.14	61.91	1.07	0.81	31.32	0.65	0.42	3.09	0.06	b.d.l	0.48	0.03	0.01	0.16	b.d.l	b.d.l	119.98	0.64	−1.81	0.02
17	+9	30–40	3.14	60.14	1.71	1.47	32.89	0.49	0.44	2.20	0.01	b.d.l	0.54	0.02	0.01	0.10	b.d.l	b.d.l	488.49	0.64	−1.65	0.02
17	+9	40–50	3.12	61.52	2.40	1.51	30.56	0.57	0.44	2.00	0.01	b.d.l	0.77	0.03	0.01	0.16	b.d.l	b.d.l	676.81	0.66	−1.58	0.03
17	+9	50–75	3.15	61.38	2.41	1.22	29.64	0.68	0.34	2.21	0.01	0.01	1.74	0.05	0.01	0.26	0.02	b.d.l	520.56	0.66	−1.45	0.06

Note: b.d.l = below detection. Soil pH was measured in 0.01 M $CaCl_2$.

$$MAT = 52.18 \times MBT_{5Me}' - 23.05 \quad (4)$$

Additionally, Bayesian regression models (BayMBT) (Dearing Crampton-Flood et al., 2020) and machine learning algorithms (FROG) (Véquaud et al., 2022) were used to investigate the relationship between brGDGTs and measured peat temperature instead of the classically applied linear regressions (see Fig. S2).

The relative abundance of 6-methyl versus 5-methyl brGDGTs (IR_{6Me}) was calculated as De Jonge et al. (2014b) (Eq. (5)):

$$IR_{6Me} = \frac{[IIa'] + [IIIa']}{[IIa] + [IIIa] + [IIa'] + [IIIa']} \quad (5)$$

The degree of cyclization of brGDGTs is captured by the cyclization of branched tetraether index (CBT′) and it was used to reconstruct soil pH as previously defined by De Jonge et al. (2014a) (Eqs. (6) and (7)).

$$CBT' = -log\frac{[Ic] + [IIa'] + [IIb'] + [IIc'] + [IIIa'] + [IIIb'] + [IIIc']}{[Ia] + [IIa] + [IIIa]} \quad (6)$$

$$pH = 7.15 + 1.59 \times CBT' \quad (7)$$

In the above equations the roman numerals refer to the different GDGT molecular structures presented by De Jonge et al. (2014a) and the square brackets indicate the fractional abundance of brGDGTs. The 6-methyl brGDGTs are denoted by an apostrophe after the Roman numerals for their corresponding 5-methyl isomers (De Jonge et al., 2014a; Naafs et al., 2017).

2.4. Data analyses

We evaluated the effects of measured soil temperature and peat depth on the abundance and distribution of brGDGTs using general linear mixed-effect models. The regression models included plot as a random effect, and all other predictor variables (soil temperature and peat depth) as fixed effects. In the models, we used the actual temperature measured at −0.3 m below the hollows averaged over the period 2016 to 2018 (Table S1). We used soil temperature measurements rather than air temperature since the offset between soil and air temperature does not contribute to significantly more accurate temperature reconstructions (see Fig. S3). We verified for bivariate relationships between all variables to ensure that a linear model was appropriate. Normality and homoscedasticity were checked in all models using residuals and Q-Q plots and adjusted when needed to fit parametric assumptions using log transformation. When significant differences among depths were detected, we conducted pairwise comparisons using Tukey's honest significant difference test.

To assess the relationship between bacterial community and brGDGTs, we compared changes in the operational taxonomic unit (OTU) distribution with those in brGDGT distributions following the approaches of Weber et al. (2018) and Liang et al. (2023) using OTUs (sequence data) produced by Wilson et al. (2021). We performed a nonmetric multidimensional scaling (NMDS) analysis (package "*vegan*") on the OTUs based on Bray-Curtis distances. The score on NMDS axis 1 were used in the follow-up analyses as an estimate of the similarity of the bacterial community composition. To further summarize the variability of brGDGT distributions, Pearson correlations were performed between brGDGT relative abundances and possible environmental predictors including soil organic carbon, nitrogen concentrations, carbon:nitrogen ratio (Ofiti et al., 2022), net primary productivity (Hanson et al., 2020), root biomass, fine-root biomass (Malhotra et al., 2020), air temperature, soil temperature, growing season temperature (temperature above freezing), volumetric water content, water table depth (Hanson et al., 2016), and bacterial community (OTUs) (Wilson et al., 2021) (Table S1, S2). We performed redundancy analysis (package "*vegan*") before constraining the fraction of the variance in brGDGTs explained by environmental variables. Only non-redundant environmental variables which carried significantly different information were selected. A principal component analysis (PCA) was conducted to visualize the variance in the standardized fractional abundance of brGDGT lipids (package "*stats*"). BrGDGT compounds that were often below detection limit (brGDGTs IIIb, IIIc, IIIb′ and IIIc′) were excluded from the PCA analysis.

Stepwise multiple linear regression with Akaike Information Criterion (AIC) as the model selection condition was used to test whether variables net primary productivity, root biomass, soil pH, volumetric water content, water table depth, and bacterial community (in addition to the mean annual soil temperature) can result in a better regression with brGDGT relative abundances. Only variables showing correlations of $p < 0.1$ were included in the model. After the establishment of regressions, candidate models were carefully investigated for collinearity among the selected predictors and assumptions of normality by calculating variance inflation factors (a cut-off value of 1 when collinearity was considered not to exist) and graphically examining plots of residuals. In the model, environmental predictors were standardized when needed to fit parametric assumptions. The global model contained the following potential explanatory variables: soil temperature, soil pH, water-table depth, and root biomass (Table S3).

Overall, the chosen level of significance was 5 % ($p < 0.05$) in all statistical tests (unless stated otherwise). All data analysis was performed using the R v.3.6.3 (R Core Team, Vienna, Austria) using the RStudio interface v. 1.2.5033 (RStudio Team, PBC, Boston, MA).

3. Results

3.1. Molecular composition of brGDGTs in response to warming

Fifteen brGDGTs were present across all samples, with brGDGTs IIIb, IIIc, IIIb′ and IIIc′ being either below detection limit or present in trace abundances (Table 1). The majority of brGDGTs were the acyclic homologues, tetramethylated (Ia) and 5-methyl penta- (IIa) and hexamethylated (IIIa) brGDGTs (up to 99 % of total brGDGTs) (Fig. 1; Fig. S1). BrGDGT Ia dominated the brGDGT distribution and showed the widest range in fractional abundance (56–72 % of total brGDGTs), while the fractional abundance of brGDGTs IIa and IIIa varied between 24–34 % and 0.9–4.5 % respectively (Fig. 1). BrGDGTs containing cyclopentane moieties (cyclic brGDGT; Ib, Ic, IIb, IIc, IIIb) as well as 6-methyl brGDGTs (IIa′, IIb′, IIc′, IIIa′, IIIc′) were less abundant than acyclic brGDGTs (Table 1; Fig. S1). We also examined the response of individual brGDGTs to increasing soil temperatures (Fig. 1). Warming altered the molecular composition of brGDGTs, although not all homologues responded in the same way (Table 1; Fig. S1). The relative abundance of acyclic brGDGT Ia increased significantly with warming in the surface peat ($r^2 = 0.29$, $p = 0.02$; 0–30 cm; Fig. 1). In contrast, the relative abundances of brGDGTs IIa and IIa′ decreased significantly with increasing temperatures in the surface peat ($r^2 = 0.23$, $p = 0.04$, and $r^2 = 0.22$, $p = 0.04$, respectively; 0–30 cm; Fig. 1), whereas the rest of brGDGT homologues did not respond significantly to warming (Fig. 1; Fig. S1). It is important to note that the relationships between brGDGTs Ia, and IIa and the soil temperature differed between 0–10, 10–20 and 20–30 cm depths (Fig. 1). Furthermore, the above responses in brGDGTs to warming were much greater in the surface peat (0–30 cm) than at deeper depths (>30 cm) (Table 1; Fig. S4). We also assessed how warming altered the summed concentrations of all brGDGTs (Fig. 2a). We observed increased concentrations of total brGDGTs under warming in the surface peat specifically at 0–10, 10–20 and 20–30 cm depths ($r^2 = 0.76$, $p = 0.03$, $r^2 = 0.65$, $p = 0.06$, and $r^2 = 0.87$, $p = 0.01$, respectively; Table 1; Fig. 2a). It is noteworthy that in addition to brGDGTs compounds, we separated and integrated 6 isoprenoid GDGT (isoGDGTs) compounds, with isoGDGT4, crenarchaeol, and cren′ being either below detection limit or present in trace abundances (Table S4). However, we did not observe significant changes in total isoGDGTs or individual isoGDGTs homologues (including isoGDGT0, isoGDGT1, isoGDGT2, and isoGDGT3) under warming (Table S4; Fig. S6). We

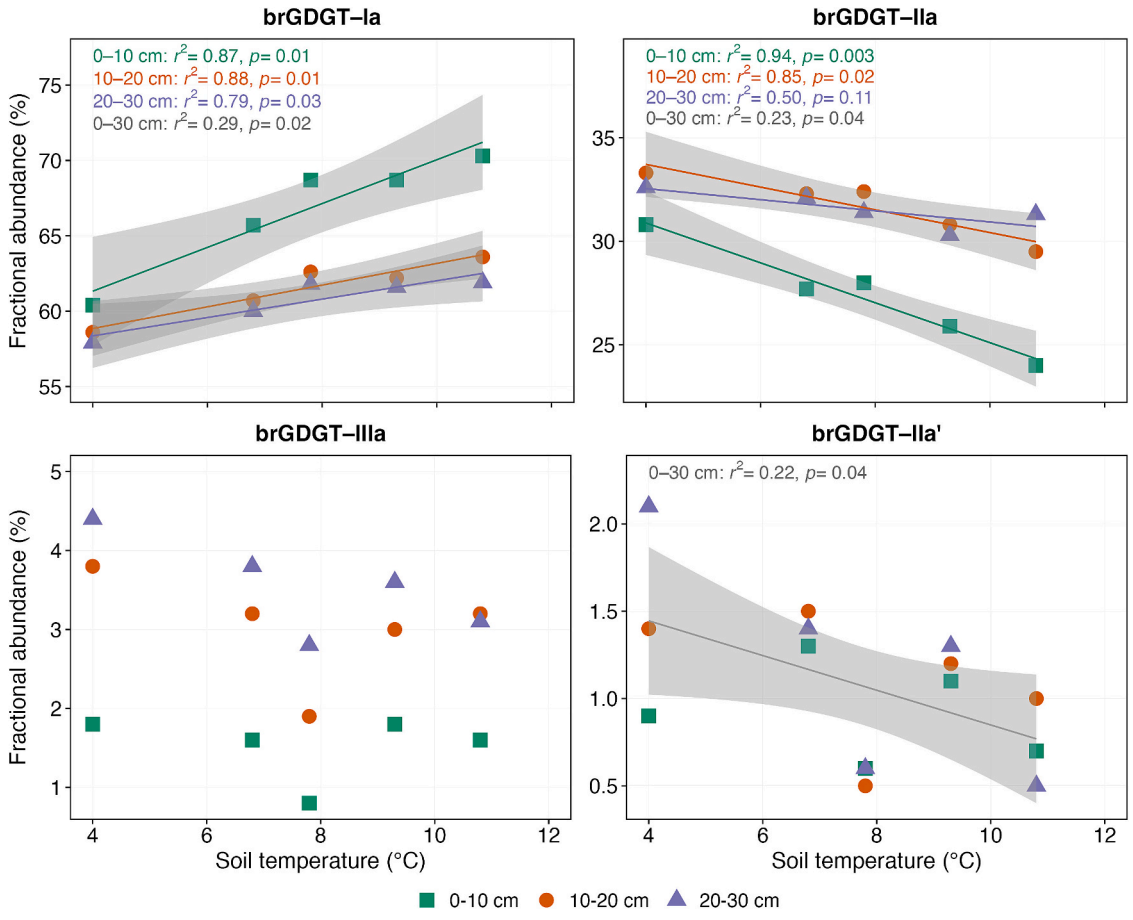

Fig. 1. Fractional abundances of selected brGDGT lipids. Relative proportion of brGDGTs Ia, IIa, IIIa and IIa′ in the surface peat (0–30 cm depth) following 4 years of warming. The fractional abundances are plotted against average soil temperature measured at 0.3 m below the hollow surface from 2016 to 2018. Depth increments are separated into statistically different groups due to a significant interaction between temperature and depth ($p < 0.05$). For instances in which differences among depths are not significant, we evaluated regression against temperature for 0–30 cm depth (regression is shown in grey). Colours represent different sampling depths; 0–10 cm (green), 10–20 cm (orange), and 20–30 cm (purple). Lines indicate significant treatment effects $p < 0.05$. Linear regression with 95 % confidence intervals is shown in grey. The absence of a line and/or confidence intervals indicates no significant trend. The roman numerals refer to the different brGDGT molecular structures presented by De Jonge et al. (2014a). Note the different y-axis scales. Also, the fractional abundances of individual brGDGT lipids in the deeper peat (>40 cm depth) did not differ significantly with increasing temperatures (see Table 1 and Supplementary Fig. S4).

further examined the response of brGDGTs to soil pH (Fig. 2b; Fig. S5). The abundance of total brGDGTs decreased significantly with increasing soil pH in the surface peat ($r^2 = 0.69$, $p = 0.00007$; 0–30 cm; Fig. 2b). However, the relative abundances of individual brGDGTs did not differ with soil pH (Fig. S5a–c).

3.2. Responses of brGDGT-based indices to warming

BrGDGT distribution was further summarized using the degree of methylation of 5-methyl (MBT'_{5Me}) and 6-methyl brGDGTs (MBT'_{6Me}), the relative abundance of 6-methyl versus 5-methyl brGDGTs (IR_{6Me}) and the cyclization index of branched tetraethers (CBT′) (Fig. 3). Variations in the abundance of individual brGDGT compounds translated into MBT'_{5Me} index which ranged between 0.61 and 0.73 and increased weakly but significantly with increasing temperature in the surface peat ($r^2 = 0.22$, $p = 0.047$; 0–30 cm; Fig. 3a). Furthermore, the MBT'_{5Me} index differed between 0–10, 10–20 and 20–30 cm depths following the warming treatment ($r^2 = 0.96$, $p = 0.002$, $r^2 = 0.89$, $p = 0.009$, and $r^2 = 0.72$, $p = 0.036$, respectively; Fig. 3a). Similarly, the MBT'_{6Me} index increased significantly with increasing temperature in the surface peat ($r^2 = 0.35$, $p = 0.01$; 0–30 cm; Fig. 3b). By contrast, the IR_{6Me} index was very low (0.02–0.06), indicating the large predominance of 5-methyl vs. 6-methyl brGDGTs, and it decreased significantly with increasing temperature in the surface peat ($r^2 = 0.26$, $p = 0.03$; 0–30 cm; Fig. 3c). The CBT′ index decreased significantly with increasing temperature in the surface peat ($r^2 = 0.27$, $p = 0.03$; 0–30 cm; Fig. 3d) but showed no variation with soil pH (Fig. S5). Notably, the MBT'_{6Me}, IR_{6Me} and CBT′ index did not differ between 0–10, 10–20 and 20–30 cm depths under warming (Fig. 3). The distinct behavior of MBT'_{5Me} values vs. depth resulted in a wide range of reconstructed temperatures (Fig. 4; Fig. S2). The reconstructed brGDGT temperature estimates generally overestimate measured soil temperature by ~4.0 °C. The MBT'_{5Me}-derived temperature estimate was 12.1 ± 2.2 °C and 10.9 ± 0.6 °C based on De Jonge et al. (2014a) and Naafs et al. (2017) calibrations respectively, whereas the average measured soil temperature value was 7.7 ± 1.2 °C (Fig. 4; Fig. S2). We note that the use of measured air temperature rather than soil temperature did not contribute to significantly more accurate temperature reconstructions (Fig. S3).

3.3. Controls on brGDGT response to warming

To further constrain the fraction of the variance in brGDGTs explained by environmental variables, brGDGT relative abundances were summarized using Pearson correlations and principal component analysis (PCA; Fig. 5). In the PCA, the two axes explained 72.1 % of the variance of brGDGT molecules (Fig. 5b). The first principal component (PC1; 44 % of variance) reflected brGDGTs Ib, Ic, IIb, and IIc, relative to the brGDGTs IIa, IIIa and IIa′. The second PC2 (28 % of variance)

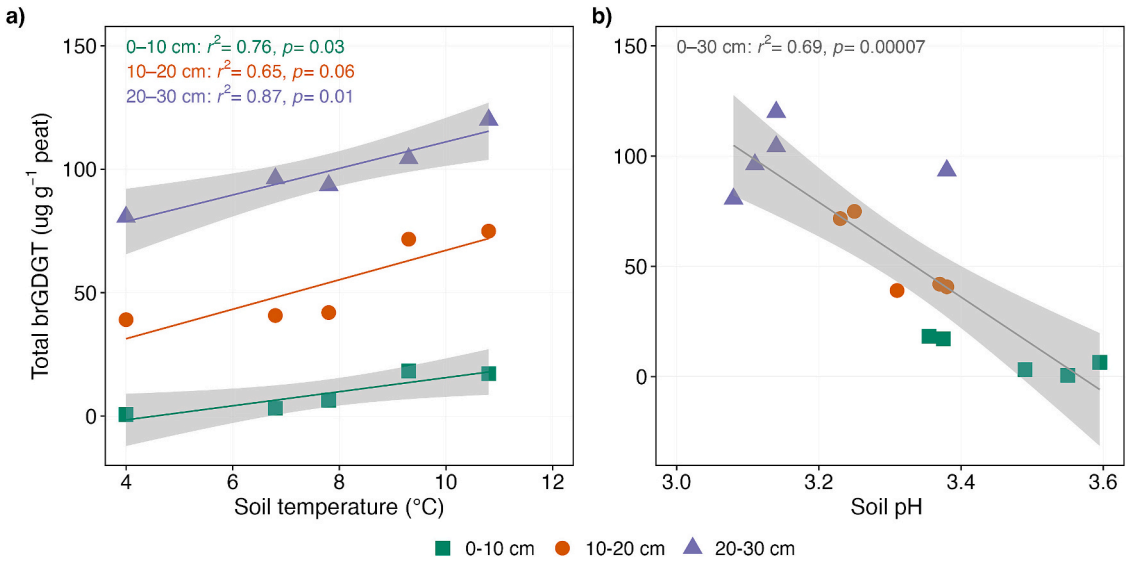

Fig. 2. The concentration of total brGDGT lipids. Scatterplot of the total sum of brGDGT compounds against a) soil temperature and b) soil pH in the surface peat following 4 years of warming. The total brGDGT lipids are plotted against average soil temperature measured at 0.3 m below the hollow surface from 2016 to 2018. Depth increments are separated into statistically different groups due to a significant interaction between temperature and depth ($p < 0.05$). For soil pH, the total sum of brGDGT compounds was evaluated against soil pH measured in 0.01 M calcium chloride solution (regression is shown in grey). Colours represent different sampling depths; 0–10 cm (green), 10–20 cm (orange), and 20–30 cm (purple). Lines indicate significant treatment effects $p < 0.05$. Linear regression with 95 % confidence intervals is shown in grey.

reflected brGDGTs Ia, IIb′, and IIc′ (Fig. 5b). Furthermore, we performed stepwise multiple linear regression model to explain dependency of brGDGTs on the environmental parameters (Fig. 5a; Table S3). Several brGDGT molecules showed significant correlations with geochemical, biological and climate variables ($p < 0.05$; Fig. 5; Table 2). We observed significant correlations between soil pH and brGDGTs IIb, and IIb′ ($p = 0.02$ and $p = 0.03$ respectively; Fig. 5a). We also obtained moderate correlations between water table depth and brGDGTs Ia ($r = 0.50$, $p = 0.01$), IIa ($r = -0.45$, $p = 0.01$), IIc ($r = -0.37$, $p = 0.03$), and IIa′ ($r = -0.50$, $p = 0.02$; Fig. 5a), whereas vegetation parameters including root biomass negatively correlated with brGDGT IIa, IIc, IIa′, IIIa′ ($p < 0.05$; Fig. 5a) whereas net primary productivity positively correlated with brGDGT IIa and IIa′ ($p < 0.05$; Fig. 5a). In an attempt to inform on the possible producers of brGDGTs, changes in the soil bacterial community composition were compared with those in brGDGTs. Previous field studies have described the microbial diversity at the SPRUCE experiment (Kolton et al., 2019; Wilson et al., 2021), with the peat microbial communities being predominated by Acidobacteria and Proteobacteria (~70 % relative abundance of overall sequence abundance), Actinobacteria (~2 %), Bacteroidetes (~2 %), Nitrospirae (~2 %), and Verrucomicrobia (~1 %). Of these phyla, only Proteobacteria and Nitrospirae showed a clear correlation with brGDGT abundances ($p < 0.05$; Fig. 6a). Among the Acidobacteria, subgroup Holophagales positively correlated with brGDGT Ia ($r = 0.58$, $p = 0.04$), but negatively correlated with brGDGTs IIb, IIIa, and IIa′ ($p < 0.05$; Fig. 6b). Similarly, subgroup Solibacterales positively correlated with brGDGTs IIb′ and IIc′ but negatively correlated with brGDGTs Ib and IIb ($p < 0.05$; Fig. 6b). We further observed significant correlations between subgroup 12 and 18 and brGDGT IIa′ ($p < 0.05$; Fig. 6b).

4. Discussion

4.1. Depth-specific response of brGDGTs to warming

The unique SPRUCE experiment enabled us to demonstrate a clear shift in the abundance and distribution of brGDGTs for an ombrotrophic peatland in a hypothetical warmer future. We observed increased concentrations of total brGDGTs and higher relative abundance of acyclic brGDGT Ia with warming, whereas the relative abundances of brGDGTs IIa, IIc and IIa′ decreased with warming in the surface peat (Figs. 1–2; Fig. S1; 0–30 cm depth). We further observed the dependency of brGDGTs on soil temperature, where the MBT'_{5Me} index increased significantly at higher temperatures (Fig. 3a; 0–30 cm depth). The more pronounced responses of brGDGTs to warming could be explained by the higher activity of brGDGT-producing bacteria with warming in the periodically aerobic surface peat (Huguet et al., 2017). At SPRUCE, the water table typically fluctuates about 10–20 cm above the hollows after snowmelt, receding deeper later in the growing season (Tfaily et al., 2014; Hobbie et al., 2016). Nevertheless, warming has resulted in a water level drawn down to about 30 cm depth (below the hollow) in the warmer plots during summer dry periods (Table S1; Hanson et al., 2020), with strong precipitation events representing the only transient perturbation to this pattern. We thus postulate that warmer temperatures did not simply induce changes in water-table depth but changed the subsurface environment from anaerobic to aerobic (oxygenated). Such changes likely created a geochemical environment that favored the production of specific brGDGT lipids (Halamka et al., 2023), the signals of which were integrated in surface aerobic layers of the acrotelm (0–30 cm depth) within a four-year timescale. In our results, water table depth was correlated with brGDGTs Ia, IIa, and IIa′ (Fig. 5; Table 2), suggesting that brGDGT production is closely related to water saturation and, in turn, likely to the oxygen content as previously suggested (Huguet et al., 2017; Halamka et al., 2021; Wu et al., 2021). However, it is worth noting that previous studies at SPRUCE have not yet observed a direct effect of warming on soil moisture (Hanson et al., 2020).

We further observed that the relationship between brGDGTs and soil temperature differed between 0–10, 10–20 and 20–30 cm depth (Figs. 1–3), likely due to changes in brGDGT-producing bacterial communities with depth and seasonal variations in water table depth (Kolton et al., 2019; Hanson et al., 2020) and thus oxidizing and reducing conditions at the respective depths (Yang et al., 2019; Pei et al., 2021). Numerous environmental studies have highlighted that brGDGTs-producing bacterial communities, and therefore brGDGT distributions can respond to variations in soil redox state and dissolved oxygen concentration (e.g., Weber et al., 2018; Wu et al., 2021). For example, Huguet et al. (2013) demonstrated how a short duration of warming (26

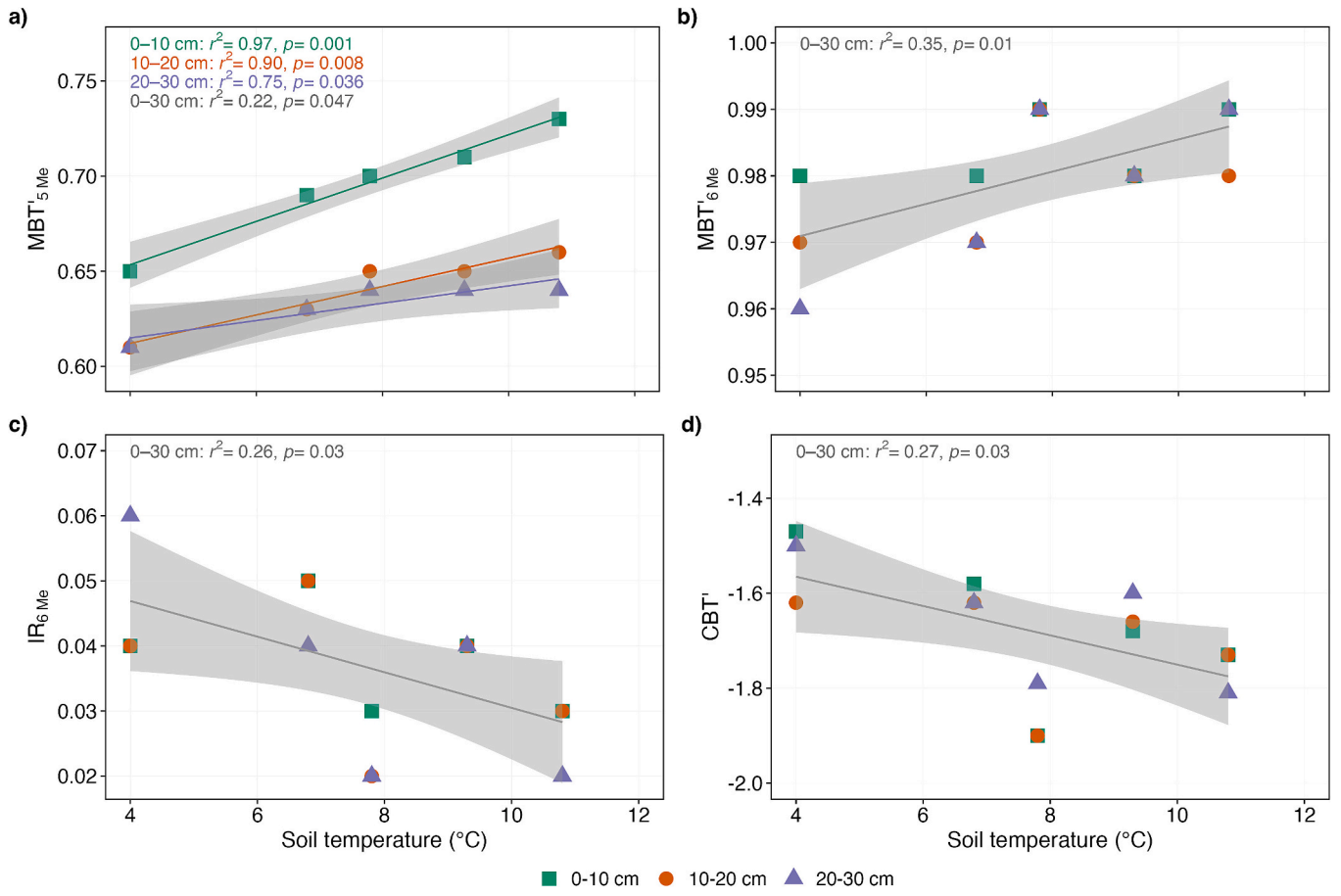

Fig. 3. BrGDGT-based temperature indices. Scatterplot of the measured soil temperature values against a) degree of methylation of 5-methyl brGDGTs (MBT'_{5Me}), b) 6-methyl brGDGTs (MBT'_{6Me}), c) the relative abundance of 6-methyl versus 5-methyl brGDGTs (IR_{6Me}) and d) the cyclization of branched tetraethers index (CBT') in the surface peat (0–30 cm depth) following 4 years of warming. BrGDGT-based indices are plotted against average soil temperature measured at 0.3 m below the hollow surface from 2016 to 2018. We evaluate regression against temperature for 0–30 cm depth (regression is shown in grey) for MBT'_{6Me}, IR_{6Me}, and CBT' because differences among depth increments were not significant. For the MBT'_{5Me}, we also evaluated regression against temperature for 0–30 cm depth (regression is shown in grey). Colours represent different sampling depths; 0–10 cm (green), 10–20 cm (orange), and 20–30 cm (purple). Lines indicate significant treatment effects $p < 0.05$. Linear regression with 95 % confidence intervals is shown in grey.

months) resulted in ~9 % increase in brGDGT Ia production in the surface peat as a result of changes in environmental conditions (at least moisture content). Our depth-specific responses of brGDGTs IIa, IIc and IIa′ (also summed concentrations of all brGDGTs) to soil warming (0–10, 10–20 and 20–30 cm; Figs. 1–3) add a new dimension to previous observations that brGDGT-producing bacteria are likely more active in surface soils exposed to warming (e.g., Huguet et al., 2013; De Jonge et al., 2019). Further, our results suggest promoted growth of brGDGT-producing bacteria communities that have varying oxygen preferences (Halamka et al., 2021), driven by low water tables and changes in bacterial community composition with depth (Wilson et al., 2016, 2021; Kolton et al., 2019; Hanson et al., 2020). However, as brGDGTs (core lipids) reflect a time-integrated signal of dead cells (fossil lipids) (Gocke et al., 2017), it is likely that different fossil lipid distributions across depths also contributed to the depth-specific responses of brGDGT to warming. Nevertheless, these findings emphasize the critical interactive impact of temperature and water level in regulating the abundance and distribution of brGDGTs in peatlands and support previous studies that hypothesized a change in the production of brGDGTs due to the growth of brGDGT source microorganisms in the periodically aerobic part of the acrotelm (e.g., Huguet et al., 2017).

We note that four years into the treatment, the abundance and distribution of brGDGTs in deeper anoxic layers of the catotelm appears largely unaltered (Fig. S4; >40 cm depth). This is likely due to a combination of limited microbial activity and slower production rate of brGDGTs in deep vs. surficial peat (Bragazza et al., 2013; Waddington et al., 2015; Huguet et al., 2017). The lower response of brGDGTs at deeper depths to warming is incongruent with the higher abundance of brGDGTs usually observed in deeper horizons of peat bogs (Weijers et al., 2006; Huguet et al., 2010), but may be explained by the retarded degradation of brGDGTs at depth and thus slower turnover under favourable, anoxic conditions (Peterse et al., 2010; Weijers et al., 2010; Huguet et al., 2013). Four years into the treatment, it remains unclear at what time-frame deeper anoxic layers of the catotelm will show significant changes in the abundance and distribution of brGDGTs. Together, our results suggest that warming induce depth-dependent brGDGT responses, which should be carefully assessed to improve our mechanistic understanding and predictions of brGDGT-based temperature proxies in peatlands.

4.2. *Influence of temperature on brGDGT concentrations and proxies*

We tested the hypothesis that warming would favour the growth of brGDGT source microorganisms, thereby enhancing the production of brGDGTs as temperatures rises (Huguet et al., 2013; Chen et al., 2018; De Jonge et al., 2019). Our results support this hypothesis and provide evidence that warmer temperatures led to changes in the fractional abundance of the three most abundant brGDGTs that determine variation in the MBT'_{5Me} (i.e., brGDGT Ia, IIa) in surface aerobic parts of the acrotelm (Figs. 1–2; Fig. S2; 0–30 cm depth). We observed increased

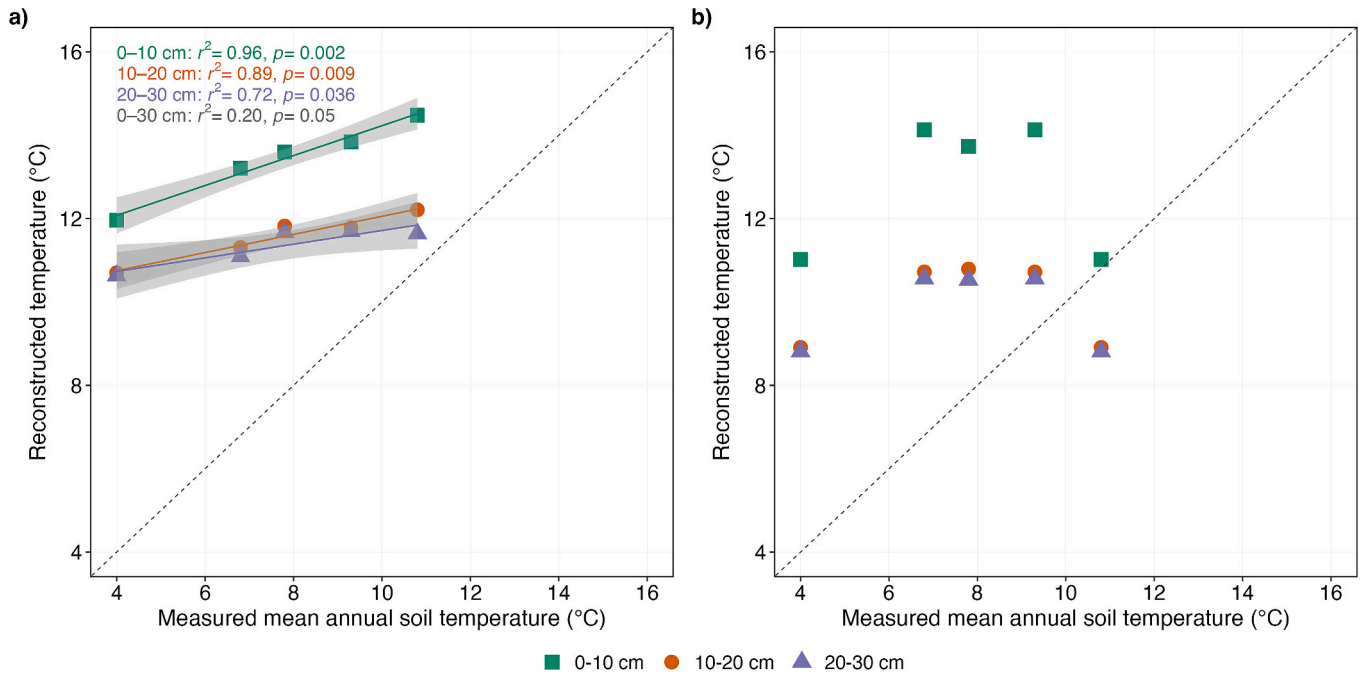

Fig. 4. BrGDGT-based temperature reconstruction. Scatterplot of the measured soil temperature values against reconstructed MBT'_{5Me}-based temperatures using global calibrations from a) De Jonge et al. (2014a) and b) Naafs et al. (2017) in the surface peat (0–30 cm depth) following 4 years of warming. BrGDGT-based reconstructions are plotted against average soil temperature measured at 0.3 m below the hollow surface from 2016 to 2018. Depth increments are separated into statistically different groups due to a significant interaction between temperature and depth ($p < 0.05$). Colours represent different sampling depths; 0–10 cm (green), 10–20 cm (orange), and 20–30 cm (purple). Lines indicate significant treatment effects $p < 0.05$. Linear regression with 95 % confidence intervals is shown in grey. The absence of a line and/or confidence intervals indicates no significant trend. The 1:1 line between reconstructed brGDGT-based temperatures and measured soil temperature is plotted with a grey dotted line. Note that we also used Bayesian statistics and machine learning algorithms (Fig. S2), measured mean annual air temperature (Fig. S3), and growing season temperature (soil temperature above 0 °C) (Fig. S7) to reconstruct MBT'_{5Me}-based temperatures.

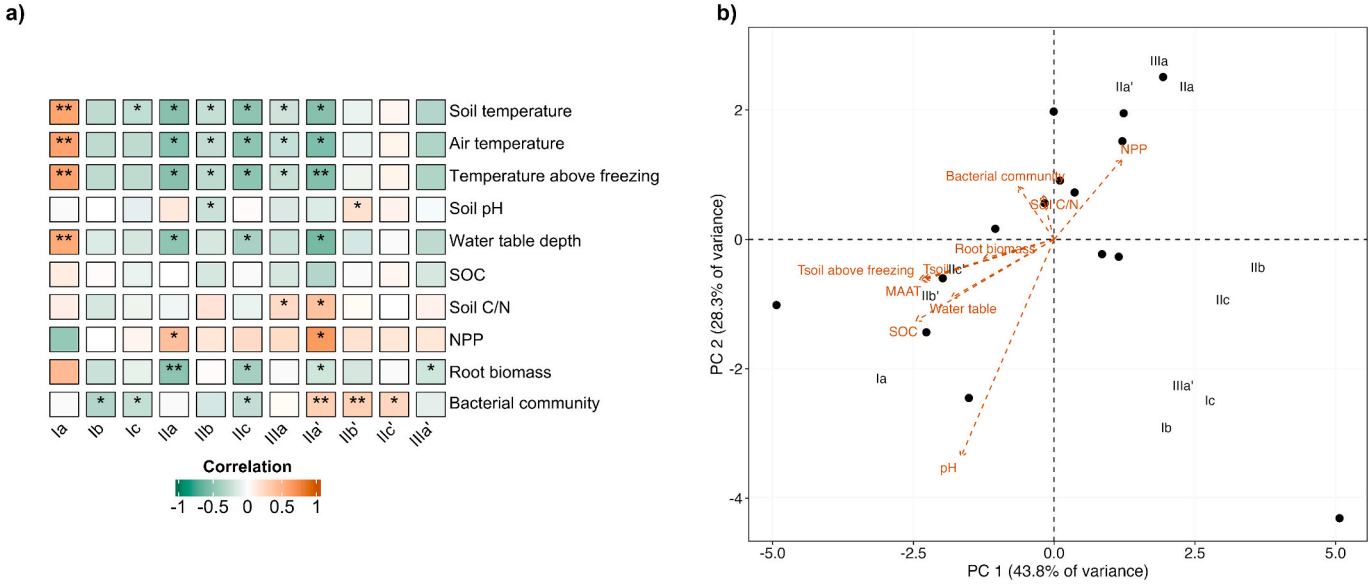

Fig. 5. Correlations (*r*) between brGDGT lipids and biogeochemical drivers. a) Pearson correlations between individual brGDGT lipids and biogeochemical predictors soil and air temperature, soil pH (Hanson et al., 2016), soil organic carbon concentration (SOC; mg g $peat^{-1}$), carbon:nitrogen ratio (C/N) (Ofiti et al., 2022), net primary productivity (NPP; g C m^{-2} $year^{-1}$) (Hanson et al., 2020), root biomass (g m^{-2}) (Malhotra et al., 2020), water table depth (maximum distance from surface to the water table; cm) (Hanson et al., 2016), and bacterial community (Wilson et al., 2021), and b) principal component (PC) analysis based on the standardized fractional abundances of 12 abundant brGDGTs in the surface peat (0–30 cm depth). The score on NMDS axis 1 (nonmetric multidimensional scaling based on Bray-Curtis distances) was used as an estimate of the similarity of the bacterial community composition. In the PC, mean annual air temperature (MAAT), soil temperature (Tsoil), temperature above freezing (Tsoil above freezing), soil pH, soil organic carbon (SOC), carbon:nitrogen ratio (soil C/N), net primary productivity (NPP), root biomass, water table depth, and bacterial community were plotted a posteriori in the ordination space. Correlated significance at $p < 0.05$ is represented with *, $p < 0.01$ is represented with **, and $p < 0.001$ is represented with ***.

Table 2
Linear correlations of brGDGT lipid indices with selected biogeochemical predictors' parameters in the surface peat (0–30 cm depth). Pearson correlations were performed between brGDGTs indices including summed concentration of all brGDGTs (μg g^{-1} soil), methylation index of C_5-methyl brGDGT (MBT'_{5Me}), the relative abundance of 6-methyl versus 5-methyl brGDGTs (IR_{6Me}) and the cyclization of branched tetraethers index (CBT′) and soil parameters (pH, water table depth, soil organic carbon, carbon:nitrogen ratio), temperature parameters (measured mean annual soil and air temperature), soil bacterial community (OTUs), and vegetation parameters (net primary productivity and fine-root biomass). The Pearson *r* - value and *p* - value are reported only for significant correlations ($p < 0.05$). In the table MAT_{rec} = reconstructed mean soil temperature and pH_{rec} = reconstructed soil pH.

		BrGDGT fractional abundance (%)										BrGDGT μg·g^{-1} soil	MBT'_{5me}	CBT′	IR'_{6me}	MAT_{rec}	pH_{rec}
		Ia	Ib	Ic	IIa	IIb	IIc	IIIa	IIa′	IIb′	IIc′	IIIa′						
Soil pH	*r*					−0.23				0.58			−0.85	0.54				
	p					0.06				<0.05			0.000	<0.05				
Air temperature	*r*	0.60			−0.52	−0.27	−0.49	−0.25	−0.53					0.52	−0.60	−0.59	0.51	−0.61
	p	<0.05			<0.05	0.05	<0.05	0.05	<0.05					<0.05	<0.05	<0.05	<0.05	<0.05
Soil temperature	*r*	0.59			−0.53	−0.25	−0.50	−0.23	−0.53					0.52	−0.57	−0.56	0.51	−0.58
	p	<0.05			<0.05	0.05	<0.05	0.05	<0.05					<0.05	<0.05	<0.05	<0.05	<0.05
Water table depth	*r*	0.50			−0.49				−0.50					0.48	−0.61	−0.65		−0.61
	p	<0.05			<0.05				<0.05					0.05	<0.05	<0.01		<0.05
Soil organic carbon	*r*																	
	p																	
Soil C/N	*r*							0.22	0.40									
	p							0.05	<0.05									
Primary productivity	*r*				0.41				0.42						0.62	0.71		0.62
	p				<0.05				<0.05						<0.01	<0.01		<0.05
Root biomass	*r*				−0.51		−0.39		−0.21			−0.20						
	p				<0.05		<0.05		0.05			0.05						
Bacteria community	*r*		−0.34	−0.25			−0.27		0.30	0.29	0.25							
	p		<0.05	<0.05			<0.05		<0.05	<0.05	<0.05							

concentrations of total brGDGTs and acyclic brGDGT Ia (Figs. 1–2), whereas 5-methyl and 6-methyl brGDGTs IIa and IIa′ decreased in concentration in warmer soils suggesting that the production of brGDGTs is linked to temperature. However, the relative abundances of monocyclic and bicyclic brGDGTs remained mostly unchanged despite temperature increases of up to +9 °C (Fig. 1; Fig. S1), likely due to their low abundances in peat soils (Naafs et al., 2017; Wei et al., 2022). While the increase in concentration of acyclic brGDGT Ia support previously observed temperature dependency of the acyclic brGDGT lipids (Weijers et al., 2007; De Jonge et al., 2014a; Naafs et al., 2017; Liang et al., 2023), our study confirms that soil brGDGTs directly respond to soil temperature variations (Huguet et al., 2013; Chen et al., 2018; De Jonge et al., 2019).

To further assess the dependency of brGDGTs on soil temperature, brGDGT distributions were translated into temperature using the classically applied MBT'_{5Me} index and the global transfer functions (De Jonge et al., 2014a; Naafs et al., 2017), as well as Bayesian regression models (BayMBT) (Dearing Crampton-Flood et al., 2020) and machine learning algorithms (FROG) (Véquaud et al., 2022). We observed a strong shift in brGDGT proxies in response to rising soil temperatures, where the MBT'_{5Me} index increased significantly at higher temperatures (Fig. 3a; Fig. S2), suggesting that warming, as expected, has a strong effect on brGDGT methylation (Naafs et al., 2017; De Jonge et al., 2019; Dearing Crampton-Flood et al., 2020). Comparison of brGDGT-derived temperatures with the measured mean annual soil temperature showed that the reconstructed temperatures follow the soil temperature gradient at SPRUCE (Fig. 4; Fig. S2). Nevertheless, the relation still had a large error. BrGDGT-based temperature reconstructions overestimated measured soil temperature to a larger extent at lower warming levels (residual error ~+6.0 °C; a warm-bias) than at higher warming levels (residual error ~+2.0 °C), which possibly reflects the heterogeneous and local response of brGDGT distribution to temperature. The observed warm-bias in reconstructed temperature at lower warming levels is larger than the current calibration errors (ca. 4 °C) (De Jonge et al., 2014a; Naafs et al., 2017; Dearing Crampton-Flood et al., 2020; Véquaud et al., 2022). The discrepancy between reconstructed and measured temperatures has been proposed to be caused by confounding factors such as the offset between soil and air temperature, seasonality, soil moisture availability, and pH (Dang et al., 2016; De Jonge et al., 2021; Halffman et al., 2022; Rao et al., 2022). The use of in situ air temperature measurements as in the global soil calibrations, rather than soil temperature data, did not substantially reduce the uncertainty associated with brGDGT-derived temperatures (Fig. S3). Furthermore, the use of peat calibration (Naafs et al., 2017) or Bayesian statistics and machine learning algorithms instead of the classically applied linear regressions (Dearing Crampton-Flood et al., 2020; Véquaud et al., 2022) did not contribute to more accurate temperature reconstructions (Fig. 4b; Fig. S4). However, removing the effect of differences in the seasonal amplitude of soil temperature and limiting the impact of frozen days (growing season temperatures; above 0 °C) seem to contribute to more accurate temperature reconstructions (residual error ~2.0 °C; Fig. S7). This suggests a higher percentage of active brGDGT-producing bacteria at higher warming levels, thus a warm-bias for reconstructed temperatures (Huguet et al., 2013; De Jonge et al., 2019; Véquaud et al., 2022). Alternatively, brGDGT production likely increases during the summer months (summer bias) (Dearing Crampton-Flood et al., 2020), particularly due to large seasonal variations in temperature at our experimental site.

It is noteworthy that we observed a significant decrease in the relative abundance of 6-methyl versus 5-methyl brGDGTs (IR_{6Me}) despite empirical investigations of peat soils showing no relationships between IR_{6Me} and temperature on a global scale (Naafs et al., 2017; Dearing Crampton-Flood et al., 2020). This decrease in IR_{6Me} should be interpreted with care given that the relation between IR_{6Me} and the measured soil temperature had a weak determination coefficient and the observed IR_{6Me} values were generally very low (on average lower than 0.05)

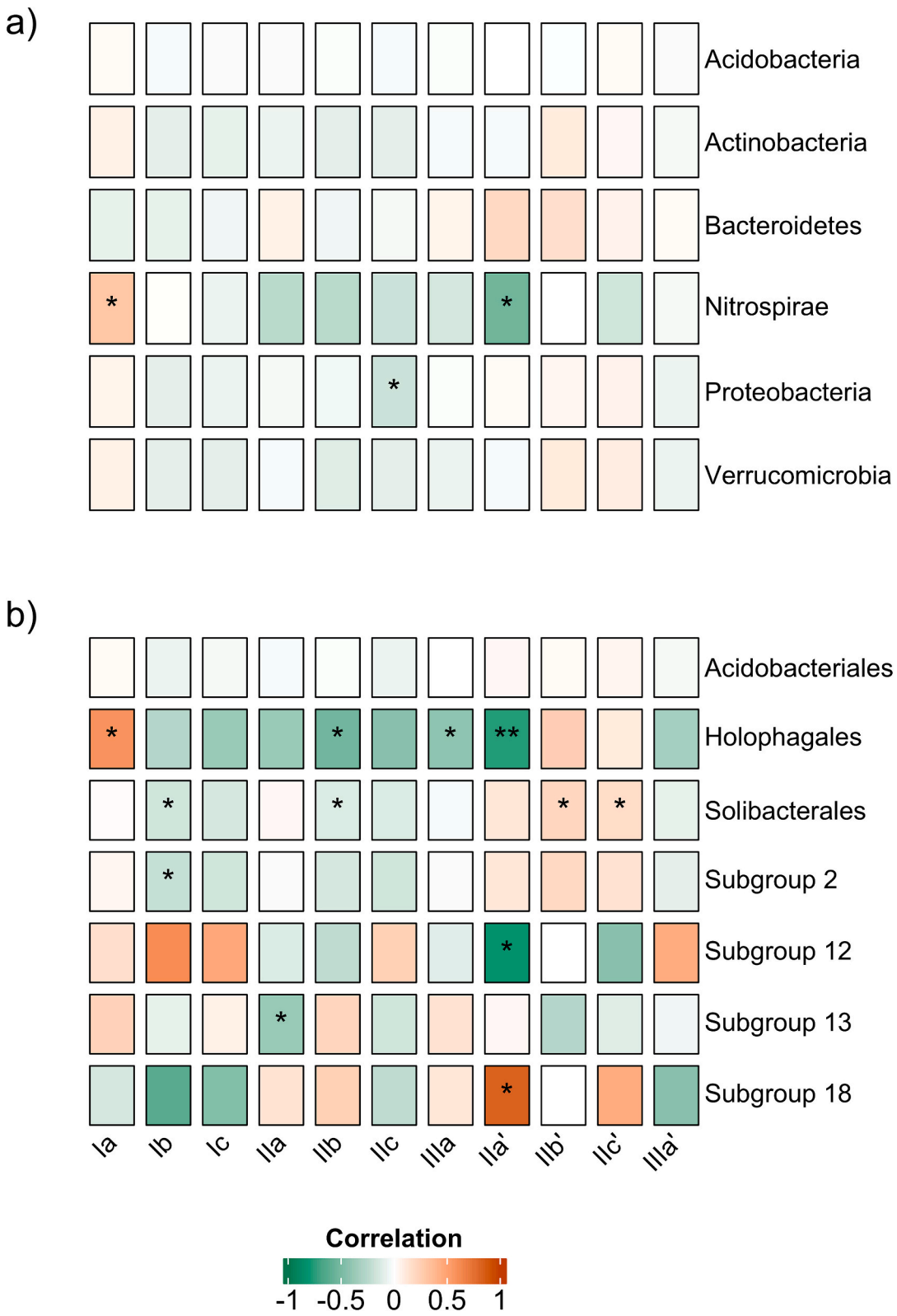

Fig. 6. Diversity of operational taxonomic units (OTUs) that have strong correlation with brGDGTs. Spearman's correlation matrix of the predominant bacterial communities with individual brGDGT lipids in the surface peat (0–30 cm depth). Highly correlated OTUs are displayed at the phylum level for Acidobacteria, Actinobacteria, Bacteroidetes, Nitrospirae, Proteobacteria, and Verrucomicrobia (a) and as subclasses of phylum Acidobacteria (b). Correlated significance at $p < 0.05$ is represented with *, $p < 0.01$ is represented with **, and $p < 0.001$ is represented with ***. The bacterial community composition datasets are derived from soil samples taken in 2016–2017 (Kolton et al., 2019; Wilson et al., 2021). Although the DNA and lipid data are derived from soil samples taken a year apart, the slow turnover time of brGDGTs should result in negligible year-to-year variation (Weijers et al., 2010; Huguet et al., 2017).

(Fig. 3c), consistent with the previously reported results for global peat soils (Naafs et al., 2017; Wei et al., 2022). These results highlight the general characteristic of peat brGDGTs as containing a minor fraction of 6-methyl brGDGTs (<1 %; Table 1), which may be the result of anoxic conditions during part of the year when the water table is very high (Hanson et al., 2020), and low soil temperature and pH in boreal peatlands (Moore and Basiliko, 2006; Waddington et al., 2015). However, it is plausible that unaccounted changes in the peat chemistry in our experiment (stronger decomposition and cycling has led to increased nitrogen and phosphorus concentration) (Iversen et al., 2022; Ofiti et al., 2023) is driving IR_{6Me} response, given that this has been observed in previous independent experiments (De Jonge et al., 2021; Halffman et al., 2022).

To further delineate the influence of temperature on GDGTs, we assessed whether temperature had an effect on the concentration and distribution of isoprenoid GDGTs (isoGDGTs). The isoprenoid GDGTs are characteristic membrane lipids of Archaea (Schouten et al., 2013), and they have been used to infer the archaeal community structure and as environmental change proxies (e.g., Coffinet et al., 2014; Yang et al., 2016; Duan et al., 2022). Although isoGDGTs were present at concentrations of 0–9500 ng g^{-1} soil, with isoGDGT4, crenarchaeol, and cren′ being either below detection limit or present in trace amounts (Table S4), the concentrations of individual isoGDGT homologues remained unaffected by warming (Table S4; Fig. S6). While these results are expected given the low abundances of isoGDGTs (Table S4), recent evidence show that temperature and/or soil moisture have potentially important effects on isoGDGTs (and proxies) on a global scale (Yang et al., 2016). To the best of our knowledge, no previous in-situ peatland manipulation studies have reported on the fate of isoGDGTs under changing environmental conditions.

4.3. Soil and environmental parameters regulate the abundance and distribution of brGDGTs

Multiplicity of environmental variables beyond soil temperature may affect the distribution of bacterial lipids, as previously shown for brGDGTs (e.g., soil moisture, seasonality, pH conditions, vegetation type, and nutrient status) (Huguet et al., 2013; Dang et al., 2016; Liang et al., 2019; Halamka et al., 2021; Guo et al., 2022; Halffman et al., 2022; Rao et al., 2022; De Jonge et al., 2024), masking or overriding relationships with temperature. We performed linear correlations and stepwise multiple linear regressions (Fig. 5; Table S3) to disentangle and quantify the main drivers of changes in brGDGT distributions. We explored the possible influence of parameters that covary with soil temperature including soil moisture availability (water-table depth), soil pH, vegetation (net primary productivity, root biomass, fine-root biomass), soil bacterial community, and nutrient status (soil organic carbon and carbon:nitrogen ratio) on brGDGT fractional abundances and distributions (Dang et al., 2016; De Jonge et al., 2019). We observed that soil temperature and water-table depth were positively correlated with brGDGT Ia (Fig. 5; Table 2), whereas soil temperature, water-table, and root biomass were significant in explaining variation in the brGDGTs IIa, IIc and IIa′ (Fig. 5; Table. S3), demonstrating that brGDGT production is closely related to the oxygen content (Dang et al., 2016; Halamka et al., 2021) and vegetation dynamics (Gocke et al., 2017; Liang et al., 2019). Furthermore, soil pH, water-table depth, root biomass and soil organic carbon were significant predictors of the variation in the MBT'_{5Me} values when considered separately but not when combined with the soil temperature (Fig. 5; Table S3). As warming was accompanied by a substantial water level drawdown during summer dry periods at our experimental site (Hanson et al., 2020), our results suggest that variation in brGDGTs is not only linked to temperature but could also result from the response of brGDGT-producing bacteria to differences in vegetation, redox condition, and water level. Our results agree with previous studies which suggested that brGDGT lipids can respond rapidly to changes in biotic and abiotic soil parameters (e.g., Liang et al., 2019, 2023; Halamka et al., 2021; Halffman et al., 2022; De Jonge et al., 2024). Hence, whereas soil temperature is the main abiotic factor influencing brGDGT production, other environmental factors beyond soil temperature have potentially important effects on the abundance and distribution of brGDGTs (Huguet et al., 2013; Chen et al., 2018; De Jonge et al., 2019).

We also assessed the dependency between soil pH and brGDGT lipids following soil warming. We observed strong negative correlations between brGDGT lipids and soil pH where total brGDGT concentration decreased with increasing soil pH (Fig. 2b), consistent with previous studies showing that brGDGT production is favored at low pH (e.g., Weijers et al., 2006). Furthermore, brGDGTs IIb and IIb′ significantly correlated with soil pH (Fig. 5a). Indeed, the stepwise multiple linear regression model revealed soil pH as one of the factors that was significant in explaining variation in brGDGTs Ia and IIa (Table S3). We also observed positive correlations between MBT'_{5Me} and soil pH, whereas CBT′ index did not correlate with soil pH (Fig. S5d–e; Table. S3), inconsistent with correlations derived from the global soil dataset (e.g., De Jonge et al., 2014a; Naafs et al., 2017). This discrepancy could be due to the low abundance of cyclopentane-containing brGDGTs used in the calculation of the CBT index and/or low pH values and range in our study (Fig. 1; Fig. S1, Table S2), which may increase the scattering of the data obtained via the pH and CBT′ relationship (Huguet et al., 2010; De Jonge et al., 2014a; Raberg et al., 2022). Additionally, our results do not support the previously observed pH dependency of the fractional abundance of 6-methyl brGDGTs (De Jonge et al., 2014a), suggesting that the widely observed environmental relationship between pH and brGDGTs through the CBT index reflect a response to other environmental parameters that co-vary with pH (Dang et al., 2016; Halffman et al., 2022; Rao et al., 2022). We propose that the very low abundances of 6-methyl brGDGTs (including cyclic) and the low range of variation in soil pH (△pH, ~0.5; Table 1) may cause the lack of pH dependency on brGDGTs and a bias in CBT-inferred pH (Fig. S5; Table S3) particularly in peatlands characterized by very low pH (Moore and Basiliko, 2006; Bragazza et al., 2013).

4.4. Bacterial metabolic response to temperature drives brGDGT composition

A key outstanding question in brGDGT proxy research is whether the empirical relationships between brGDGTs and temperature correspond to membrane adaptation and/or community changes of brGDGT source organisms to changing environment (Weijers et al., 2007; Liang et al., 2019; Véquaud et al., 2021; Halffman et al., 2022; Raberg et al., 2022). However, these hypotheses to-date remain impossible to ascertain as brGDGT source organisms remain incompletely identified and cultured (Halamka et al., 2023). In an attempt to identify potential producers of brGDGTs, we compared changes in bacterial community composition (operational taxonomic unit (OTU) distribution) with those in brGDGT distributions (Fig. 6). Similar to previous studies (e.g., Guo et al., 2022; Liang et al., 2023), we observed correlations between brGDGT lipids and OTUs belonging to phylum Acidobacteria where subgroup Holophagales significantly correlated with brGDGTs Ia, IIb, IIIa, and IIa′, whereas Solibacterales correlated with brGDGTs Ib, IIb, IIb′ and IIc′, while Subgroup 2, 12, and 13 significantly correlated with brGDGTs Ib, IIa′, and IIa respectively (Fig. 6b). So far, phylum Acidobacteria is considered to provide some of the potential source organisms of GDGTs as they have been shown to produce brGDGTs and/or precursor lipids (Sinninghe Damsté et al., 2011; Halamka et al., 2021; Chen et al., 2022; Zeng et al., 2022). Our results thus confirm phylum Acidobacteria as a good candidate for containing brGDGT producers. Of the other five main phyla present in our samples, only Proteobacteria and Nitrospirae showed a clear correlation with brGDGT abundances (Fig. 6a). Phylum Nitrospirae was positively correlated with brGDGT Ia but negatively correlated with brGDGT IIa′, whereas phylum Proteobacteria was negatively correlated with brGDGT IIc (Fig. 6a). Although we cannot

verify that these bacterial phyla are brGDGT-producers, our results suggest that along with Acidobacteria, members of the Proteobacteria and Nitrospirae possibly contribute to brGDGT production. It is important to note that neither phyla Acidobacteria, Proteobacteria and Nitrospirae nor their subgroups showed a clear temperature dependency in this experiment (Wilson et al., 2016, 2021; Kolton et al., 2019), which is what we would expect if the relationship between brGDGTs and temperature corresponds to community changes of brGDGT source organisms (De Jonge et al., 2019; Wu et al., 2021). As the bacterial community composition remained largely unaltered, our results suggests that physiological adaptation of the bacteria producing these lipids resulted in altered brGDGT abundances with increasing temperatures (Weijers et al., 2007; Naafs et al., 2021; Véquaud et al., 2021). This further suggests that physiological plasticity resulted in an increase in MBT'_{5Me} in our study. However, this does not exclude the fact that in other settings and sites the change in bacterial communities may explain at least a part of the changes in brGDGT distribution (Weber et al., 2018; De Jonge et al., 2019; Wu et al., 2021).

We posit three hypotheses to explain correlations between brGDGTs and phyla Acidobacteria, Proteobacteria and Nitrospirae under warming (Fig. 6) despite an absence of a temperature response within the bacterial communities. The first hypothesis is that other bacterial phyla could possibly also contain brGDGT producing organisms. Although the Acidobacteria is currently the only phylum that has been shown to produce brGDGTs and/or precursor lipids (Sinninghe Damsté et al., 2011; Halamka et al., 2021; Chen et al., 2022; Zeng et al., 2022), it is unlikely that the same species synthesize brGDGTs in all types of terrestrial (and aquatic) settings (Sinninghe Damsté et al., 2018). The distinct responses of 5 vs. 6-methyl brGDGTs to temperature (Fig. 1; Fig. S1) agrees with the suggestion that they may be produced by different bacterial phyla (Sinninghe Damsté et al., 2018; Weber et al., 2018; De Jonge et al., 2019; Martínez-Sosa et al., 2020). This could also explain the larger diversity of brGDGT compounds encountered in the environment ($n = 15$), compared to only the 5-methyl brGDGTs that have been so far detected in two strains of Acidobacteria cultures in vitro (Chen et al., 2022; Halamka et al., 2023). However, we cannot rule out that responses of 5 vs. 6-methyl brGDGTs to temperature could also be due to the low abundance of 6-methyl brGDGTs in peat soils (Huguet et al., 2010; De Jonge et al., 2014a; Raberg et al., 2022). Secondly, either the source organisms of brGDGTs in peat are low abundant members of the bacterial community or brGDGTs constitute only a small fraction of the microbial cell membranes, consistent with the lipid profile of certain Acidobacteria (Sinninghe Damsté et al., 2011). In this study, brGDGTs were only actively altered in the surface layers under periodically oxic conditions (Figs. 1–4). BrGDGT source organisms are thus presumably aerobes or facultative aerobes (Huguet et al., 2017) that are not the dominant members of the peat bacterial community as previously suggested (Weijers et al., 2009). They may have been selected for in the surface peat by fluctuation in the water table. Third, there might be temporal offsets between the responses captured by brGDGT lipid pool (i.e., core lipid) and a more recent bacterial DNA signature (Gocke et al., 2017). Studies have shown that changes in bacterial community composition can occur over a few years to decades of warming (DeAngelis et al., 2015; Oliverio et al., 2017; Romero-Olivares et al., 2017), whereas brGDGT lipids integrate microbial and environmental processes on decadal time scales (Weijers et al., 2010; Huguet et al., 2013, 2017). Thus, the observed shifts in brGDGTs under warming probably reflect a transient adjustment period to the application of the experimental treatments, where microbial growth and traits have not yet reached a new equilibrium (Ofiti et al., 2022). A more detailed look at the phylogenetic nature of the shift in the bacterial community coupled with core lipid brGDGTs (evaluated here) and intact polar lipids, the latter being assumed to derive from living cells and thus more freshly produced (Gocke et al., 2017; Naafs et al., 2019), is needed to validate these hypotheses. Nevertheless, we propose that the dependency of brGDGTs on soil temperature is caused by the interplay between physiological adaptation and the direct impact of environmental factors.

4.5. Implications for brGDGT-based indices for climate reconstructions

The unique setup of increasing temperatures at the SPRUCE experiment enabled us to quantify changes in brGDGT abundance and distribution to reveal mechanisms of the dependency of brGDGT on soil temperature in a boreal peatland. We demonstrate that under scenarios of water table drawdown, the resulting aerobic conditions and higher summer temperatures could cause substantial shifts in brGDGT fingerprint (abundance and distribution), at least in the short term. Specifically, MBT'_{5Me} responded to the climate-induced warming, whereas brGDGT-based temperature reconstructions overestimated (residual error ~+6.0 °C) the measured soil temperature in our experiment (Figs. 3a, 4). However, removing the effect of differences in the seasonal amplitude of soil temperature contributed to more accurate temperature reconstructions (residual error ~+2.0 °C; Fig. S7), highlighting a warm bias for reconstructed temperatures (Huguet et al., 2013; De Jonge et al., 2019; Véquaud et al., 2022). Our results thus indicate that a moderate increase in temperature can be reconstructed using the MBT'_{5Me} index. The relatively high activity of brGDGT source organisms in the surface peat (acrotelm; 0–30 cm depth) and the associated rapid turnover of brGDGTs argue for fast response of the surface peat, and thus these biomarkers integrate microbial and environmental processes on short time scales (less than a decade) (Huguet et al., 2017; De Jonge et al., 2019). The strong link between the composition of the bacterial community and brGDGT lipids (Fig. 5a, 6), in combination with the non-uniform response of potential brGDGT source organisms to temperature in our experiment (Kolton et al., 2019; Wilson et al., 2021), tentatively confirms that physiological adaptation of the microorganisms producing these lipids is partly responsible for brGDGT responses to changes in temperature in this boreal peatland. Although we observed pH dependency of the fractional abundance of brGDGT compounds such as IIb, and IIb′ (Fig. 5), the CBT′ index did not correlate with soil pH, likely due to the low pH values and the low range of variation in soil pH (△pH, ~0.5; Fig. 2; Fig. S5; Table S2), which might have increased the scattering of the data obtained via the pH and CBT′ relationship. We propose that in soils with low pH (~3.0), and low abundances of cyclic brGDGTs, the relationship between soil pH and CBT′ index and their dependencies should be interpreted with caution as being uniquely driven by soil pH.

Collectively, our study provides evidence that the MBT'_{5Me} index can't be used as reliable temperature reconstructions proxy, at least at this site ($r^2 = 0.22$, $p = 0.047$; Fig. 3a), despite the fractional abundance of the three most abundant brGDGTs that determine variation in the MBT'_{5Me}, correlating moderately to strongly with temperature. We thus defined an alternate local scale transfer function based on a linear combination of the fractional abundance of brGDGT compounds (Eq. (8); Fig. 7):

$$\mathrm{MAT} = -38.23 - 8.69 \times [\mathrm{IIc}] - 1.31 \times [\mathrm{IIa}] + 2.40 \times [\mathrm{IIIa}] + 0.65 \times [\mathrm{Ia}] + 4.26 \times [\mathrm{Ic}] \quad (8)$$

Testing the performance of this new calibration, we observed that the site-specific calibration had a much higher determination coefficient and lower RMSE than the global transfer functions derived from the MBT'_{5Me}-temperature relationship (Fig. 7c; $n = 30$, RMSE = 1.63 °C, $r^2 = 0.50$, $p = 0.003$). Crucially, these results suggest that brGDGTs can be used for temperature reconstructions even in highly diverse and contrasted environments such as boreal peatlands. Nevertheless, the implication for the use of brGDGTs as paleoclimate proxy is that reconstructed temperature should be interpreted with caution, as changes in environmental factors beyond temperature could strongly affect brGDGTs production and therefore a change in the brGDGT signature.

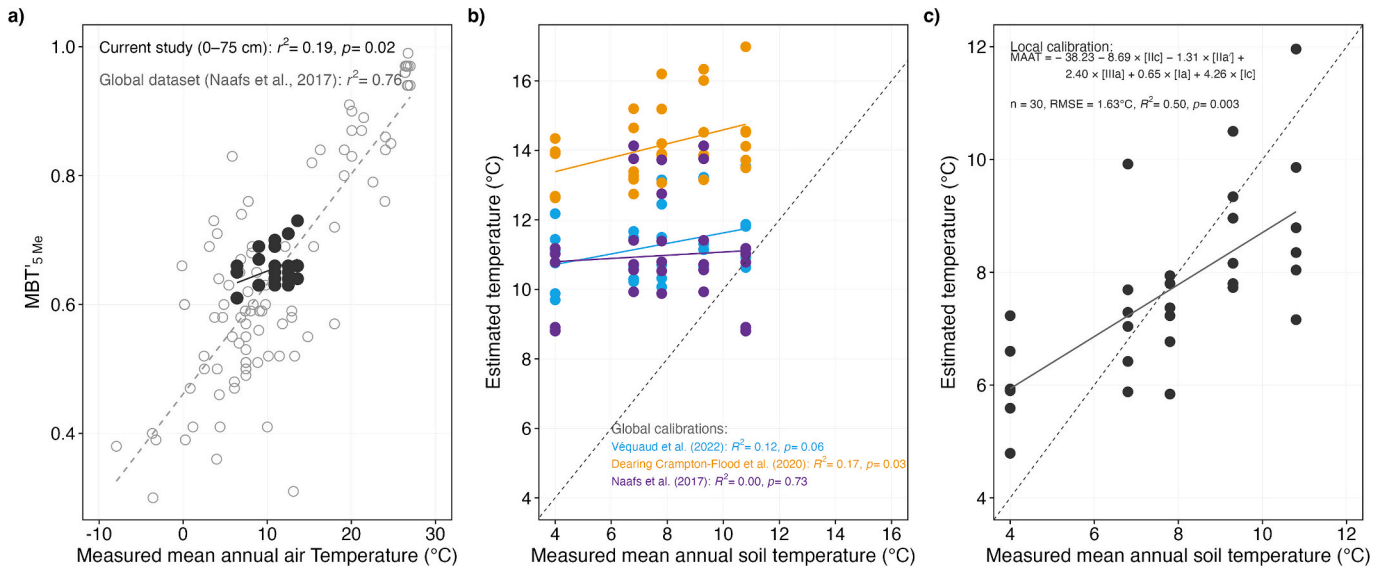

Fig. 7. BrGDGT-based temperature reconstruction. Scatterplot of the a) measured mean annual air temperature against MBT'_{5Me} values for soils in the global peat dataset from Naafs et al. (2017) with samples of the global peat dataset in grey and samples of the current study in black (0–75 cm depth; black line indicate correlations of the current study, the dotted line indicates the correlation for the whole dataset), b) reconstructed MBT'_{5Me}-based temperatures against measured mean annual soil temperature for 0–75 cm depth using global linear calibrations (Naafs et al., 2017), Bayesian statistics (Dearing Crampton-Flood et al., 2020), and machine learning algorithms (Véquaud et al., 2022) (colours represent different global calibrations), and c) mean annual soil temperature estimated using new local-scale calibration based on a linear combination of the fractional abundance of brGDGT compounds (Eq. (6)) vs. measured mean annual soil temperature observed at SPRUCE (0–75 cm depth; black line indicate correlations) following 4 years of warming. The Roman numerals correspond to the different brGDGT structures presented in De Jonge et al. (2014a). The 1:1 line between reconstructed brGDGT-based temperatures and measured soil temperature is plotted with a grey dotted line.

While our results indicate that warming and associated water table drawdown are the primarily responsible factors for the variability of brGDGTs lipids (Fig. 5; Table S3), it remains to be seen whether brGDGT abundance and distribution in deeper anoxic layers of the catotelm will be responsive to prolonged warming and extended water-table drawdown. Furthermore, we do not know whether brGDGT signatures will be affected in the long-run by changes in plant and microbial community composition as they adapt to warmer temperatures. It is therefore important to complement our results with long-term, time-resolved analyses, and to implement our results into revised parameterizations of brGDGT-based temperature models. Another missing piece in our study is a more detailed assessment of intact polar lipids (IPLs), assumed to derive from living bacteria lipids and thus more freshly produced, and brGDGTs (assessed in the current study), the latter being assumed to derive from "fossil" lipid pool and a more recent warming-induced lipid pool (Gocke et al., 2017). The assessment of IPLs is a crucial step in unravelling whether the responses of brGDGTs to temperature might be caused by the varying "fossil" brGDGT distributions preserved at different depths, with an ultimate goal of improving the accuracy of brGDGT-based proxies. In the meantime, however, our results provide evidence that warming may favour the growth of brGDGT source microorganisms and enhance the production of brGDGTs as temperatures rise. We also highlight a rapid renewal of brGDGTs in response to four years of warming, consistent with previous studies in peat soils showing that the turnover of brGDGTs is in the range of 8–41 years (Huguet et al., 2013). The relatively high activity of brGDGT source organisms (Huguet et al., 2017; De Jonge et al., 2019) and the associated rapid turnover of brGDGTs suggest that brGDGTs, and thus studies that implement these biomarkers, integrate microbial and environmental processes on short time scales (less than a decade) in peatland environments.

5. Conclusion

Future climate warming is expected to directly affect carbon cycling in peatlands by provoking a series of responses including changes to the community of microorganisms as well as their physiology. Understanding the future dynamics of these ecosystems is possible from studying their Holocene history and previous response to environmental perturbations. Using one of the first longest running in situ peatland climate change experiment, we quantified changes in brGDGTs, classically used for understanding past environmental changes, to reveal mechanisms of climate change responses in a boreal peatland. Our unique ecosystem scale study provides experimental evidence for the direct effect of temperature on brGDGT lipids. We demonstrated that under scenarios of water table drawdown, the resulting aerobic conditions, and warmer temperatures could cause a rapid turnover of brGDGT lipids, indicating that the paleoenvironmental signal recorded in peatland environments can be altered on short time scales (within a four-year timescale). Furthermore, we revealed that brGDGT distributions differed between individual soil depths, highlighting depth-specific response of brGDGT lipids to warming, which should be considered in paleoenvironmental studies. This depth-specific response of brGDGTs to warming reflected changes in brGDGT source organisms and seasonal variations in water table and thus oxidizing and reducing conditions at each depth. As the bacterial community composition was generally unaltered, the rapid changes in brGDGTs rather imply a physiological adaptation of the microorganisms producing these lipids, driven by environmental and biotic factors. To conclude, our results reveal new insights on depth-specific response of brGDGTs and predominance of physiological adaptation of brGDGT-producing bacteria to environmental changes, and underscores brGDGT as viable paleo-temperature proxies for better understanding of climatic perturbation in peatlands.

Funding

The Swiss National Science Foundation (SNF) grant, awarded to the DEEP C project (project 200021_172744), and the U.S. Department of Energy Office of Science, Office of Biological and Environmental Research Terrestrial Ecosystem Science Program, through support for the Oak Ridge National Laboratory which is managed by UT-Battelle,

LLC, for the US DOE under Contract DE-AC05-00OR22725, and Swiss Academy of Engineering Sciences (SATW) for funding of the Germaine de Stael project 2019/08 "The consequence of future soil warming on carbon cycling at a molecular level". N. Ofiti acknowledges funding from the Swiss National Science Foundation (Postdoc mobility grant P500PN_206708).

CRediT authorship contribution statement

Nicholas O.E. Ofiti: Conceptualization, Formal analysis, Funding acquisition, Investigation, Visualization, Writing – original draft, Writing – review & editing. **Arnaud Huguet:** Conceptualization, Funding acquisition, Methodology, Resources, Validation, Writing – review & editing. **Paul J. Hanson:** Data curation, Funding acquisition, Resources, Writing – review & editing. **Guido L.B. Wiesenberg:** Conceptualization, Funding acquisition, Resources, Validation, Writing – review & editing.

Declaration of competing interest

The authors declare that they have no known competing financial interests or personal relationships that could have appeared to influence the work reported in this paper.

Data access

The data used in this study will be available in the online project archive at https://mnspruce.ornl.gov and the long-term storage in the U. S. Department of Energy's Environmental Systems Science Data Infrastructure for a Virtual Ecosystem (ESS-DIVE; https://ess-dive. lbl.gov).

Acknowledgements

We thank E. Solly for field assistance, and C. Zosso for inspiration. We also thank C. Anquetil for LC-MS analyses. We would like to thank anonymous reviewers for their constructive feedback that improved the manuscript.

Appendix A. Supplementary data

Supplementary data to this article can be found online at https://doi.org/10.1016/j.scitotenv.2024.171666.

References

Bradford, M.A., Wieder, W.R., Bonan, G.B., Fierer, N., Raymond, P.A., Crowther, T.W., 2016. Managing uncertainty in soil carbon feedbacks to climate change. Nat. Clim. Chang. 6, 751.

Bragazza, L., Parisod, J., Buttler, A., Bardgett, R.D., 2013. Biogeochemical plant-soil microbe feedback in response to climate warming in peatlands. Nat. Clim. Chang. 3, 273–277. https://doi.org/10.1038/nclimate1781.

Bridgham, S.D., Patrick, Megonigal, J., Keller, J.K., Bliss, N.B., Trettin, C., 2006. The carbon balance of North American wetlands. In: Wetlands 2006 26:4. Springer. https://doi.org/10.1672/0277-5212(2006)26[889:TCBONA]2.0.CO;2.

Bucher, M., Ofiti, N.O.E., Malhotra, A., 2023. Plant functional types and microtopography mediate climate change responses of fine roots in forested boreal peatlands. Front. For. Glob. Change 6, 90. https://doi.org/10.3389/FFGC.2023.1170252.

Charman, D.J., Beilman, D.W., Blaauw, M., Booth, R.K., Brewer, S., Chambers, F.M., Christen, J.A., Gallego-Sala, A., Harrison, S.P., Hughes, P.D.M., Jackson, S.T., Korhola, A., Mauquoy, D., Mitchell, F.J.G., Prentice, I.C., Van Der Linden, M., De Vleeschouwer, F., Yu, Z.C., Alm, J., Bauer, I.E., Corish, Y.M.C., Garneau, M., Hohl, V., Huang, Y., Karofeld, E., Le Roux, G., Loisel, J., Moschen, R., Nichols, J.E., Nieminen, T.M., MacDonald, G.M., Phadtare, N.R., Rausch, N., Sillasoo, U., Swindles, G.T., Tuittila, E.S., Ukonmaanaho, L., Väliranta, M., Van Bellen, S., Van Geel, B., Vitt, D.H., Zhao, Y., 2013. Climate-related changes in peatland carbon accumulation during the last millennium. Biogeosciences 10, 929–944. https://doi.org/10.5194/BG-10-929-2013.

Chaudhary, N., Westermann, S., Lamba, S., Shurpali, N., Sannel, A.B.K., Schurgers, G., Miller, P.A., Smith, B., 2020. Modelling past and future peatland carbon dynamics across the pan-Arctic. Glob. Chang. Biol. 26, 4119–4133. https://doi.org/10.1111/GCB.15099.

Chen, Y., Zheng, F., Chen, S., Liu, H., Phelps, T.J., Zhang, C., 2018. Branched GDGT production at elevated temperatures in anaerobic soil microcosm incubations. Org. Geochem. 117, 12–21. https://doi.org/10.1016/J.ORGGEOCHEM.2017.11.015.

Chen, Y., Zheng, F., Yang, H., Yang, W., Wu, R., Liu, X., Liang, H., Chen, H., Pei, H., Zhang, C., Pancost, R.D., Zeng, Z., 2022. The production of diverse brGDGTs by an Acidobacterium providing a physiological basis for paleoclimate proxies. Geochim. Cosmochim. Acta. https://doi.org/10.1016/J.GCA.2022.08.033.

Coffinet, S., Huguet, A., Williamson, D., Fosse, C., Derenne, S., 2014. Potential of GDGTs as a temperature proxy along an altitudinal transect at Mount Rungwe (Tanzania). Org. Geochem. 68, 82–89. https://doi.org/10.1016/J.ORGGEOCHEM.2014.01.004.

Coffinet, S., Huguet, A., Bergonzini, L., Pedentchouk, N., Williamson, D., Anquetil, C., Gałka, M., Kołaczek, P., Karpińska-Kołaczek, M., Majule, A., Laggoun-Défarge, F., Wagner, T., Derenne, S., 2018. Impact of climate change on the ecology of the Kyambangunguru crater marsh in southwestern Tanzania during the Late Holocene. Quat. Sci. Rev. 196, 100–117. https://doi.org/10.1016/J.QUASCIREV.2018.07.038.

Dang, X., Yang, H., Naafs, B.D.A., Pancost, R.D., Xie, S., 2016. Evidence of moisture control on the methylation of branched glycerol dialkyl glycerol tetraethers in semi-arid and arid soils. Geochim. Cosmochim. Acta 189, 24–36. https://doi.org/10.1016/J.GCA.2016.06.004.

De Jonge, C., Hopmans, E.C., Stadnitskaia, A., Rijpstra, W.I.C., Hofland, R., Tegelaar, E., Sinninghe Damsté, J.S., 2013. Identification of novel penta- and hexamethylated branched glycerol dialkyl glycerol tetraethers in peat using HPLC–MS2, GC–MS and GC–SMB-MS. Org. Geochem. 54, 78–82. https://doi.org/10.1016/J.ORGGEOCHEM.2012.10.004.

De Jonge, C., Hopmans, E.C., Zell, C.I., Kim, J.H., Schouten, S., Sinninghe Damsté, J.S., 2014a. Occurrence and abundance of 6-methyl branched glycerol dialkyl glycerol tetraethers in soils: implications for palaeoclimate reconstruction. Geochim. Cosmochim. Acta 141, 97–112. https://doi.org/10.1016/J.GCA.2014.06.013.

De Jonge, C., Stadnitskaia, A., Hopmans, E.C., Cherkashov, G., Fedotov, A., Sinninghe Damsté, J.S., 2014b. In situ produced branched glycerol dialkyl glycerol tetraethers in suspended particulate matter from the Yenisei River, Eastern Siberia. Geochim. Cosmochim. Acta 125, 476–491. https://doi.org/10.1016/J.GCA.2013.10.031.

De Jonge, C., Radujković, D., Sigurdsson, B.D., Weedon, J.T., Janssens, I., Peterse, F., 2019. Lipid biomarker temperature proxy responds to abrupt shift in the bacterial community composition in geothermally heated soils. Org. Geochem. 137, 103897 https://doi.org/10.1016/J.ORGGEOCHEM.2019.07.006.

De Jonge, C., Kuramae, E.E., Radujković, D., Weedon, J.T., Janssens, I.A., Peterse, F., 2021. The influence of soil chemistry on branched tetraether lipids in mid- and high latitude soils: implications for brGDGT- based paleothermometry. Geochim. Cosmochim. Acta 310, 95–112. https://doi.org/10.1016/J.GCA.2021.06.037.

De Jonge, C., Guo, J., Hällberg, P., Griepentrog, M., Rifai, H., Richter, A., Ramirez, E., Zhang, X., Smittenberg, R.H., Peterse, F., Boeckx, P., Dercon, G., 2024. The impact of soil chemistry, moisture and temperature on branched and isoprenoid GDGTs in soils: a study using six globally distributed elevation transects. Org. Geochem. 187, 104706 https://doi.org/10.1016/J.ORGGEOCHEM.2023.104706.

DeAngelis, K.M., Pold, G., Topcuoglu, B.D., van Diepen, L.T.A., Varney, R.M., Blanchard, J.L., Melillo, J., Frey, S.D., 2015. Long-term forest soil warming alters microbial communities in temperate forest soils. Front. Microbiol. 6 https://doi.org/10.3389/fmicb.2015.00104. ARTN 104.

Dearing Crampton-Flood, E., Tierney, J.E., Peterse, F., Kirkels, F.M.S.A., Sinninghe Damsté, J.S., 2020. BayMBT: a Bayesian calibration model for branched glycerol dialkyl glycerol tetraethers in soils and peats. Geochim. Cosmochim. Acta 268, 142–159. https://doi.org/10.1016/J.GCA.2019.09.043.

Duan, Y., Sun, Q., Werne, J.P., Hou, J., Yang, H., Wang, Q., Khormali, F., Xia, D., Chu, G., Chen, F., 2022. General Holocene warming trend in arid Central Asia indicated by soil isoprenoid tetraethers. Glob. Planet. Chang. 215, 103879 https://doi.org/10.1016/J.GLOPLACHA.2022.103879.

Gallego-Sala, A.V., Charman, D.J., Brewer, S., Page, S.E., Prentice, I.C., Friedlingstein, P., Moreton, S., Amesbury, M.J., Beilman, D.W., Björck, S., Blyakharchuk, T., Bochicchio, C., Booth, R.K., Bunbury, J., Camill, P., Carless, D., Chimner, R.A., Clifford, M., Cressey, E., Courtney-Mustaphi, C., De Vleeschouwer, F., de Jong, R., Fialkiewicz-Koziel, B., Finkelstein, S.A., Garneau, M., Githumbi, E., Hribjlan, J., Holmquist, J., Hughes, P.D.M., Jones, C., Jones, M.C., Karofeld, E., Klein, E.S., Kokfelt, U., Korhola, A., Lacourse, T., Le Roux, G., Lamentowicz, M., Large, D., Lavoie, M., Loisel, J., Mackay, H., MacDonald, G.M., Makila, M., Magnan, G., Marchant, R., Marcisz, K., Martínez Cortizas, A., Massa, C., Mathijssen, P., Mauquoy, D., Mighall, T., Mitchell, F.J.G., Moss, P., Nichols, J., Oksanen, P.O., Orme, L., Packalen, M.S., Robinson, S., Roland, T.P., Sanderson, N.K., Sannel, A.B.K., Silva-Sánchez, N., Steinberg, N., Swindles, G.T., Turner, T.E., Uglow, J., Väliranta, M., van Bellen, S., van der Linden, M., van Geel, B., Wang, G., Yu, Z., Zaragoza-Castells, J., Zhao, Y., 2018. Latitudinal limits to the predicted increase of the peatland carbon sink with warming. Nat. Clim. Chang. 8, 907–913. https://doi.org/10.1038/s41558-018-0271-1.

Gauthier, S., Bernier, P., Kuuluvainen, T., Shvidenko, A.Z., Schepaschenko, D.G., 2015. Boreal forest health and global change. Science 349, 819–822. https://doi.org/10.1126/science.aaa9092.

Gill, A.L., Giasson, M.-A., Yu, R., Finzi, A.C., 2017. Deep peat warming increases surface methane and carbon dioxide emissions in a black spruce-dominated ombrotrophic bog. Glob. Chang. Biol. 23, 5398–5411. https://doi.org/10.1111/gcb.13806.

Gocke, M.I., Huguet, A., Derenne, S., Kolb, S., Dippold, M.A., Wiesenberg, G.L.B., 2017. Disentangling interactions between microbial communities and roots in deep subsoil. Sci. Total Environ. 575, 135–145. https://doi.org/10.1016/J.SCITOTENV.2016.09.184.

Gorham, E., 1991. Northern peatlands: role in the carbon cycle and probable responses to climatic warming. Ecol. Appl. 1, 182–195. https://doi.org/10.2307/1941811.

Guo, J., Ma, T., Liu, N., Zhang, X., Hu, H., Ma, W., Wang, Z., Feng, X., Peterse, F., 2022. Soil pH and aridity influence distributions of branched tetraether lipids in grassland soils along an aridity transect. Org. Geochem. 164, 104347 https://doi.org/10.1016/J.ORGGEOCHEM.2021.104347.

Häggi, C., Naafs, B.D.A., Silvestro, D., Bertassoli, D.J., Akabane, T.K., Mendes, V.R., Sawakuchi, A.O., Chiessi, C.M., Jaramillo, C.A., Feakins, S.J., 2023. GDGT distribution in tropical soils and its potential as a terrestrial paleothermometer revealed by Bayesian deep-learning models. Geochim. Cosmochim. Acta 362, 41–64. https://doi.org/10.1016/J.GCA.2023.09.014.

Halamka, T.A., McFarlin, J.M., Younkin, A.D., Depoy, J., Dildar, N., Kopf, S.H., 2021. Oxygen limitation can trigger the production of branched GDGTs in culture. Geochem. Perspect. Lett. 19, 36–39. https://doi.org/10.7185/GEOCHEMLET.2132.

Halamka, T.A., Raberg, J.H., McFarlin, J.M., Younkin, A.D., Mulligan, C., Liu, X.L., Kopf, S.H., 2023. Production of diverse brGDGTs by Acidobacterium Solibacter usitatus in response to temperature, pH, and O_2 provides a culturing perspective on brGDGT proxies and biosynthesis. Geobiology 21, 102–118. https://doi.org/10.1111/GBI.12525.

Halffman, R., Lembrechts, J., Radujković, D., De Gruyter, J., Nijs, I., De Jonge, C., 2022. Soil chemistry, temperature and bacterial community composition drive brGDGT distributions along a subarctic elevation gradient. Org. Geochem. 163, 104346 https://doi.org/10.1016/J.ORGGEOCHEM.2021.104346.

Hanson, P.J., Riggs, J.S., Robert Nettles, W., Krassovski, M.B., Hook, L.A., 2016. SPRUCE Whole Ecosystems Warming (WEW) Environmental Data Beginning August 2015. Department of Energy, Oak Ridge, Tennessee, U.S.A, Oak Ridge National Laboratory, TES SFA, U.S.

Hanson, P.J., Riggs, J.S., Robert Nettles, W., Phillips, J.R., Krassovski, M.B., Hook, L.A., Gu, L., Richardson, A.D., Aubrecht, D.M., Ricciuto, D.M., Warren, J.M., Barbier, C., 2017. Attaining whole-ecosystem warming using air and deep-soil heating methods with an elevated CO_2 atmosphere. Biogeosciences 14, 861–883. https://doi.org/10.5194/bg-14-861-2017.

Hanson, P.J., Griffiths, N.A., Iversen, C.M., Norby, R.J., Sebestyen, S.D., Phillips, J.R., Chanton, J.P., Kolka, R.K., Malhotra, A., Oleheiser, K.C., Warren, J.M., Shi, X., Yang, X., Mao, J., Ricciuto, D.M., 2020. Rapid net carbon loss from a whole-ecosystem warmed peatland. AGU Adv. 1 https://doi.org/10.1029/2020AV000163.

Hobbie, E.A., Chen, J., Hanson, P.J., Iversen, C.M., McFarlane, K.J., Thorp, N.R., Hofmockel, K.S., 2016. Long-term carbon and nitrogen dynamics at SPRUCE revealed through stable isotopes in peat profiles. Biogeosci. Discuss. 1–23 https://doi.org/10.5194/bg-2016-261.

Hopmans, E.C., Schouten, S., Sinninghe Damsté, J.S., 2016. The effect of improved chromatography on GDGT-based palaeoproxies. Org. Geochem. 93, 1–6. https://doi.org/10.1016/J.ORGGEOCHEM.2015.12.006.

Huguet, A., Fosse, C., Laggoun-Défarge, F., Toussaint, M.L., Derenne, S., 2010. Occurrence and distribution of glycerol dialkyl glycerol tetraethers in a French peat bog. Org. Geochem. 41, 559–572. https://doi.org/10.1016/J.ORGGEOCHEM.2010.02.015.

Huguet, A., Fosse, C., Laggoun-Défarge, F., Delarue, F., Derenne, S., 2013. Effects of a short-term experimental microclimate warming on the abundance and distribution of branched GDGTs in a French peatland. Geochim. Cosmochim. Acta 105, 294–315. https://doi.org/10.1016/J.GCA.2012.11.037.

Huguet, A., Meador, T.B., Laggoun-Défarge, F., Könneke, M., Wu, W., Derenne, S., Hinrichs, K.U., 2017. Production rates of bacterial tetraether lipids and fatty acids in peatland under varying oxygen concentrations. Geochim. Cosmochim. Acta 203, 103–116. https://doi.org/10.1016/J.GCA.2017.01.012.

Huguet, A., Coffinet, S., Roussel, A., Gayraud, F., Anquetil, C., Bergonzini, L., Bonanomi, G., Williamson, D., Majule, A., Derenne, S., 2019. Evaluation of 3-hydroxy fatty acids as a pH and temperature proxy in soils from temperate and tropical altitudinal gradients. Org. Geochem. 129, 1–13. https://doi.org/10.1016/J.ORGGEOCHEM.2019.01.002.

Iversen, C.M., Childs, J., Norby, R.J., Ontl, T.A., Kolka, R.K., Brice, D.J., McFarlane, K.J., Hanson, P.J., 2018. Fine-root growth in a forested bog is seasonally dynamic, but shallowly distributed in nutrient-poor peat. Plant Soil 424, 123–143. https://doi.org/10.1007/s11104-017-3231-z.

Iversen, C.M., Latimer, J., Brice, D.J., Childs, J., Vander Stel, H.M., Defrenne, C.E., Graham, J., Griffiths, N.A., Malhotra, A., Norby, R.J., Oleheiser, K.C., Phillips, J.R., Salmon, V.G., Sebestyen, S.D., Yang, X., Hanson, P.J., 2022. Whole-ecosystem warming increases plant-available nitrogen and phosphorus in an ombrotrophic bog. Ecosystems 2022, 1–28. https://doi.org/10.1007/S10021-022-00744-X.

Kolton, M., Marks, A., Wilson, R.M., Chanton, J.P., Kostka, J.E., 2019. Impact of warming on greenhouse gas production and microbial diversity in anoxic peat from a Sphagnum-dominated bog (Grand Rapids, Minnesota, United States). Front. Microbiol. 10, 870. https://doi.org/10.3389/fmicb.2019.00870.

Liang, J., Russell, J.M., Xie, H., Lupien, R.L., Si, G., Wang, J., Hou, J., Zhang, G., 2019. Vegetation effects on temperature calibrations of branched glycerol dialkyl glycerol tetraether (brGDGTs) in soils. Org. Geochem. 127, 1–11. https://doi.org/10.1016/J.ORGGEOCHEM.2018.10.010.

Liang, J., Richter, N., Xie, H., Zhao, B., Si, G., Wang, J., Hou, J., Zhang, G., Russell, J.M., 2023. Branched glycerol dialkyl glycerol tetraether (brGDGT) distributions influenced by bacterial community composition in various vegetation soils on the Tibetan Plateau. Palaeogeogr. Palaeoclimatol. Palaeoecol. 611, 111358 https://doi.org/10.1016/J.PALAEO.2022.111358.

Malhotra, A., Brice, D.J., Childs, J., Graham, J.D., Hobbie, E.A., Vander Stel, H., Feron, S.C., Hanson, P.J., Iversen, C.M., 2020. Peatland warming strongly increases fine-root growth. Proc. Natl. Acad. Sci. 117, 202003361 https://doi.org/10.1073/pnas.2003361117.

Martínez-Sosa, P., Tierney, J.E., Meredith, L.K., 2020. Controlled lacustrine microcosms show a brGDGT response to environmental perturbations. Org. Geochem. 145, 104041 https://doi.org/10.1016/J.ORGGEOCHEM.2020.104041.

McFarlane, K.J., Hanson, P.J., Iversen, C.M., Phillips, J.R., Brice, D.J., 2018. Local spatial heterogeneity of holocene carbon accumulation throughout the peat profile of an ombrotrophic northern Minnesota bog. Radiocarbon 60, 941–962. https://doi.org/10.1017/rdc.2018.37.

Moore, T., Basiliko, N., 2006. Decomposition in boreal peatlands. In: Boreal Peatland Ecosystems. Springer, Berlin Heidelberg, pp. 125–143. https://doi.org/10.1007/978-3-540-31913-9_7.

Naafs, B.D.A., Inglis, G.N., Zheng, Y., Amesbury, M.J., Biester, H., Bindler, R., Blewett, J., Burrows, M.A., del Castillo Torres, D., Chambers, F.M., Cohen, A.D., Evershed, R.P., Feakins, S.J., Gałka, M., Gallego-Sala, A., Gandois, L., Gray, D.M., Hatcher, P.G., Honorio Coronado, E.N., Hughes, P.D.M., Huguet, A., Könönen, M., Laggoun-Défarge, F., Lähteenoja, O., Lamentowicz, M., Marchant, R., McClymont, E., Pontevedra-Pombal, X., Ponton, C., Pourmand, A., Rizzuti, A.M., Rochefort, L., Schellekens, J., De Vleeschouwer, F., Pancost, R.D., 2017. Introducing global peat-specific temperature and pH calibrations based on brGDGT bacterial lipids. Geochim. Cosmochim. Acta 208, 285–301. https://doi.org/10.1016/J.GCA.2017.01.038.

Naafs, B.D.A., Inglis, G.N., Blewett, J., McClymont, E.L., Lauretano, V., Xie, S., Evershed, R.P., Pancost, R.D., 2019. The potential of biomarker proxies to trace climate, vegetation, and biogeochemical processes in peat: a review. Glob. Planet. Chang. https://doi.org/10.1016/j.gloplacha.2019.05.006.

Naafs, B.D.A., Oliveira, A.S.F., Mulholland, A.J., 2021. Molecular dynamics simulations support the hypothesis that the brGDGT paleothermometer is based on homeoviscous adaptation. Geochim. Cosmochim. Acta 312, 44–56. https://doi.org/10.1016/J.GCA.2021.07.034.

Nichols, J.E., Peteet, D.M., Moy, C.M., Castañeda, I.S., McGeachy, A., Perez, M., 2014. Impacts of climate and vegetation change on carbon accumulation in a south-central Alaskan peatland assessed with novel organic geochemical techniques. The Holocene 24, 1146–1155. https://doi.org/10.1177/0959683614540729.

Ofiti, N.O.E., Solly, E.F., Hanson, P.J., Malhotra, A., Wiesenberg, G.L.B., Schmidt, M.W.I., 2022. Warming and elevated CO_2 promote rapid incorporation and degradation of plant-derived organic matter in an ombrotrophic peatland. Glob. Chang. Biol. 28, 883–898. https://doi.org/10.1111/GCB.15955.

Ofiti, N.O.E., Schmidt, M.W.I., Abiven, S., Hanson, P.J., Iversen, C.M., Wilson, R.M., Kostka, J.E., Wiesenberg, G.L.B., Malhotra, A., 2023. Climate warming and elevated CO_2 alter peatland soil carbon sources and stability. Nat. Commun. 14, 1–10. https://doi.org/10.1038/s41467-023-43410-z, 2023. 1 14.

Oliverio, A.M., Bradford, M.A., Fierer, N., 2017. Identifying the microbial taxa that consistently respond to soil warming across time and space. Glob. Chang. Biol. 23, 2117–2129. https://doi.org/10.1111/gcb.13557.

Pancost, R.D., Baas, M., Van Geel, B., Sinninghe Damsté, J.S., 2002. Biomarkers as proxies for plant inputs to peats: an example from a sub-boreal ombrotrophic bog. Org. Geochem. 33, 675–690. https://doi.org/10.1016/S0146-6380(02)00048-7.

Parsekian, A.D., Slater, L., Ntarlagiannis, D., Nolan, J., Sebesteyen, S.D., Kolka, R.K., Hanson, P.J., 2012. Uncertainty in peat volume and soil carbon estimated using ground-penetrating radar and probing. Soil Sci. Soc. Am. J. 76, 1911–1918. https://doi.org/10.2136/sssaj2012.0040.

Pei, H., Zhao, S., Yang, H., Xie, S., 2021. Variation of branched tetraethers with soil depth in relation to non-temperature factors: implications for paleoclimate reconstruction. Chem. Geol. 572, 120211 https://doi.org/10.1016/J.CHEMGEO.2021.120211.

Peterse, F., Schouten, S., van der Meer, J., van der Meer, M.T.J., Sinninghe Damsté, J.S., 2009. Distribution of branched tetraether lipids in geothermally heated soils: implications for the MBT/CBT temperature proxy. Org. Geochem. 40, 201–205. https://doi.org/10.1016/J.ORGGEOCHEM.2008.10.010.

Peterse, F., Nicol, G.W., Schouten, S., Sinninghe Damsté, J.S., 2010. Influence of soil pH on the abundance and distribution of core and intact polar lipid-derived branched GDGTs in soil. Org. Geochem. 41, 1171–1175. https://doi.org/10.1016/J.ORGGEOCHEM.2010.07.004.

Raberg, J.H., Miller, G.H., Geirsdóttir, Á., Sepúlveda, J., 2022. Near-universal trends in brGDGT lipid distributions in nature. Sci. Adv. 8, 7625. https://doi.org/10.1126/SCIADV.ABM7625/SUPPL_FILE/SCIADV.ABM7625_DATA_S1.ZIP.

Rao, Z., Wei, S., Li, Y., Guo, H., Chen, F., 2021. Cooling or warming climatic background for the expansion of human activity in arid inland China and the Tibetan Plateau over the past ~4000 years? Sci. Bull. 66, 1936–1938. https://doi.org/10.1016/J.SCIB.2021.06.004.

Rao, Z., Guo, H., Wei, S., Cao, J., Jia, G., 2022. Influence of water conditions on peat brGDGTs: a modern investigation and its paleoclimatic implications. Chem. Geol. 606 https://doi.org/10.1016/j.chemgeo.2022.120993.

Romero-Olivares, A.L., Allison, S.D., Treseder, K.K., 2017. Soil microbes and their response to experimental warming over time: a meta-analysis of field studies. Soil Biol. Biochem. https://doi.org/10.1016/j.soilbio.2016.12.026.

Schouten, S., Hopmans, E.C., Sinninghe Damsté, J.S., 2013. The organic geochemistry of glycerol dialkyl glycerol tetraether lipids: a review. Org. Geochem. 54, 19–61. https://doi.org/10.1016/J.ORGGEOCHEM.2012.09.006.

Sebestyen, S.D., Dorrance, C., Olson, D.M., Verry, E.S., Kolka, R.K., Elling, A.E., Kyllander, R., 2011. Long-term monitoring sites and trends at the Marcell Experimental Forest. In: Kolka, R.K., Sebestyen, S.D., Verry, E.S., Brooks, K.N. (Eds.), Peatland Biogeochemistry and Watershed Hydrology at the Marcell Experimental Forest. *CRC Press*, pp. 15–71 (2011).

Sinninghe Damste, J.S., Hopmans, E.C., Pancost, R.D., Schouten, S., Geenevasen, J.A.J., 2000. Newly discovered non-isoprenoid glycerol dialkylglycerol tetraether lipids in sediments. Chem. Commun. 9, 1683–1684. https://doi.org/10.1039/B004517I.

Sinninghe Damsté, J.S., Rijpstra, W.I.C., Hopmans, E.C., Weijers, J.W.H., Foesel, B.U., Overmann, J., Dedysh, S.N., 2011. 13,16-Dimethyl octacosanedioic acid (iso-Diabolic Acid), a common membrane-spanning lipid of Acidobacteria subdivisions 1 and 3. Appl. Environ. Microbiol. 77, 4147–4154.

Sinninghe Damsté, J.S., Rijpstra, W.I.C., Foesel, B.U., Huber, K.J., Overmann, J., Nakagawa, S., Kim, J.J., Dunfield, P.F., Dedysh, S.N., Villanueva, L., 2018. An overview of the occurrence of ether- and ester-linked iso-diabolic acid membrane lipids in microbial cultures of the Acidobacteria: implications for brGDGT paleoproxies for temperature and pH. Org. Geochem. 124, 63–76. https://doi.org/10.1016/J.ORGGEOCHEM.2018.07.006.

Tfaily, M.M., Cooper, W.T., Kostka, J.E., Chanton, P.R., Schadt, C.W., Hanson, P.J., Iversen, C.M., Chanton, J.P., 2014. Organic matter transformation in the peat column at Marcell experimental forest: Humification and vertical stratification. J. Geophys. Res. Biogeosci. 119, 661–675. https://doi.org/10.1002/2013JG002492.

Véquaud, P., Derenne, S., Anquetil, C., Collin, S., Poulenard, J., Sabatier, P., Huguet, A., 2021. Influence of environmental parameters on the distribution of bacterial lipids in soils from the French Alps: implications for paleo-reconstructions. Org. Geochem. 153, 104194 https://doi.org/10.1016/J.ORGGEOCHEM.2021.104194.

Véquaud, P., Thibault, A., Derenne, S., Anquetil, C., Collin, S., Contreras, S., Nottingham, A.T., Sabatier, P., Werne, J.P., Huguet, A., 2022. FROG: a global machine-learning temperature calibration for branched GDGTs in soils and peats. Geochim. Cosmochim. Acta 318, 468–494. https://doi.org/10.1016/J.GCA.2021.12.007.

Waddington, J.M., Morris, P.J., Kettridge, N., Granath, G., Thompson, D.K., Moore, P.A., 2015. Hydrological feedbacks in northern peatlands. Ecohydrology 8, 113–127. https://doi.org/10.1002/ECO.1493.

Weber, Y., Damsté, J.S.S., Zopfi, J., De Jonge, C., Gilli, A., Schubert, C.J., Lepori, F., Lehmann, M.F., Niemann, H., 2018. Redox-dependent niche differentiation provides evidence for multiple bacterial sources of glycerol tetraether lipids in lakes. Proc. Natl. Acad. Sci. 115, 10926–10931. https://doi.org/10.1073/PNAS.1805186115/SUPPL_FILE/PNAS.1805186115.SD02.XLS.

Wei, S., Guo, H., Cao, J., Jia, G., Chen, M., Rao, Z., 2022. In-situ provenance of brGDGTs in peat sediments: a case study from southern China and a comparison of global results. Org. Geochem. 167, 104373 https://doi.org/10.1016/J.ORGGEOCHEM.2022.104373.

Weijers, J.W.H., Schouten, S., Hopmans, E.C., Geenevasen, J.A.J., David, O.R.P., Coleman, J.M., Pancost, R.D., Sinninghe Damsté, J.S., 2006. Membrane lipids of mesophilic anaerobic bacteria thriving in peats have typical archaeal traits. Environ. Microbiol. 8, 648–657. https://doi.org/10.1111/J.1462-2920.2005.00941.X.

Weijers, J.W.H., Schouten, S., van den Donker, J.C., Hopmans, E.C., Sinninghe Damsté, J.S., 2007. Environmental controls on bacterial tetraether membrane lipid distribution in soils. Geochim. Cosmochim. Acta 71, 703–713. https://doi.org/10.1016/J.GCA.2006.10.003.

Weijers, J.W.H., Panoto, E., van Bleijswijk, J., Schouten, S., Rijpstra, W.I.C., Balk, M., Stams, A.J.M., Damsté, J.S.S., 2009. Constraints on the biological source(s) of the orphan branched tetraether membrane lipids. Geomicrobiol J. 26, 402–414. https://doi.org/10.1080/01490450902937293.

Weijers, J.W.H., Wiesenberg, G.L.B., Bol, R., Hopmans, E.C., Pancost, R.D., 2010. Carbon isotopic composition of branched tetraether membrane lipids in soils suggest a rapid turnover and a heterotrophic life style of their source organism(s). Biogeosciences 7, 2959–2973. https://doi.org/10.5194/BG-7-2959-2010.

Wiesenberg, G.L.B., Gocke, M.I., 2017. Analysis of lipids and polycyclic aromatic hydrocarbons as indicators of past and present (micro)biological activity. In: McGenity, T.J., Timmis, K.N., Nogales, B. (Eds.), Hydrocarbon and Lipid Microbiology Protocols: Petroleum, Hydrocarbon and Lipid Analysis. Springer, Berlin Heidelberg, Berlin, Heidelberg, pp. 61–91. https://doi.org/10.1007/8623_2015_157.

Wilson, R.M., Hopple, A.M., Tfaily, M.M., Sebestyen, S.D., Schadt, C.W., Pfeifer-Meister, L., Medvedeff, C., Mcfarlane, K.J., Kostka, J.E., Kolton, M., Kolka, R.K., Kluber, L.A., Keller, J.K., Guilderson, T.P., Griffiths, N.A.A., Chanton, J.P., Bridgham, S.D., Hanson, P.J., Sebestyen, S.D., Schadt, C.W., Pfeifer-Meister, L., Medvedeff, C., Mcfarlane, K.J., Kostka, J.E., Kolton, M., Kolka, R.K., Kluber, L.A., Keller, J.K., Guilderson, T.P., Griffiths, N.A.A., Chanton, J.P., Bridgham, S.D., Hanson, P.J., 2016. Stability of peatland carbon to rising temperatures. Nat. Commun. 7, 1–10. https://doi.org/10.1038/ncomms13723.

Wilson, R.M., Tfaily, M.M., Kolton, M., Johnston, E.R., Petro, C., Zalman, C.A., Hanson, P.J., Heyman, H.M., Kyle, J.E., Hoyt, D.W., Eder, E.K., Purvine, S.O., Kolka, R.K., Sebestyen, S.D., Griffiths, N.A., Schadt, C.W., Keller, J.K., Bridgham, S.D., Chanton, J.P., Kostka, J.E., 2021. Soil metabolome response to whole-ecosystem warming at the spruce and peatland responses under changing environments experiment. Proc. Natl. Acad. Sci. U. S. A. 118 https://doi.org/10.1073/PNAS.2004192118.

Wu, J., Yang, H., Pancost, R.D., Naafs, B.D.A., Qian, S., Dang, X., Sun, H., Pei, H., Wang, R., Zhao, S., Xie, S., 2021. Variations in dissolved O2 in a Chinese lake drive changes in microbial communities and impact sedimentary GDGT distributions. Chem. Geol. 579, 120348 https://doi.org/10.1016/J.CHEMGEO.2021.120348.

Yang, H., Pancost, R.D., Jia, C., Xie, S., 2016. The response of archaeal tetraether membrane lipids in surface soils to temperature: a potential paleothermometer in paleosols. Geomicrobiol J. 33, 98–109. https://doi.org/10.1080/01490451.2014.1002956.

Yang, H., Xiao, W., Słowakiewicz, M., Ding, W., Ayari, A., Dang, X., Pei, H., 2019. Depth-dependent variation of archaeal ether lipids along soil and peat profiles from southern China: implications for the use of isoprenoidal GDGTs as environmental tracers. Org. Geochem. 128, 42–56. https://doi.org/10.1016/J.ORGGEOCHEM.2018.12.009.

Yu, Z., Loisel, J., Brosseau, D.P., Beilman, D.W., Hunt, S.J., 2010. Global peatland dynamics since the Last Glacial Maximum. Geophys. Res. Lett. 37 https://doi.org/10.1029/2010GL043584.

Yu, Z.C., 2012. Northern peatland carbon stocks and dynamics: a review. Biogeosciences 9, 4071–4085. https://doi.org/10.5194/bg-9-4071-2012.

Zeng, Z., Chen, H., Yang, H., Chen, Y., Yang, W., Feng, X., Pei, H., Welander, P.V., 2022. Identification of a protein responsible for the synthesis of archaeal membrane-spanning GDGT lipids. Nat. Commun. 13, 1–9. https://doi.org/10.1038/s41467-022-29264-x, 2022. 1 13.

Zheng, Y., Li, Q., Wang, Z., Naafs, B.D.A., Yu, X., Pancost, R.D., 2015. Peatland GDGT records of Holocene climatic and biogeochemical responses to the Asian Monsoon. Org. Geochem. 87, 86–95. https://doi.org/10.1016/J.ORGGEOCHEM.2015.07.012.